



HAL
open science

Thrust to transpression and transtension tectonics during the Paleoproterozoic evolution of the Birimian Greenstone Belt of Mako, Kédougou-Kéniéba Inlier, Eastern Senegal

Moussa Dabo, Tahar Aifa, Ibrahima Gassama, Papa Malick Ngom

► **To cite this version:**

Moussa Dabo, Tahar Aifa, Ibrahima Gassama, Papa Malick Ngom. Thrust to transpression and transtension tectonics during the Paleoproterozoic evolution of the Birimian Greenstone Belt of Mako, Kédougou-Kéniéba Inlier, Eastern Senegal. *Journal of African Earth Sciences*, 2018, 148, pp.14-29. 10.1016/j.jafrearsci.2018.05.010 . insu-01803991

HAL Id: insu-01803991

<https://insu.hal.science/insu-01803991>

Submitted on 31 May 2018

HAL is a multi-disciplinary open access archive for the deposit and dissemination of scientific research documents, whether they are published or not. The documents may come from teaching and research institutions in France or abroad, or from public or private research centers.

L'archive ouverte pluridisciplinaire **HAL**, est destinée au dépôt et à la diffusion de documents scientifiques de niveau recherche, publiés ou non, émanant des établissements d'enseignement et de recherche français ou étrangers, des laboratoires publics ou privés.

Accepted Manuscript

Revised version Thrust tectonics and transtension tectonics during the Paleoproterozoic evolution of the Birimian Greenstone Belt of Mako, Kédougou-Kéniéba Inlier, Eastern Senegal



Moussa Dabo, Tahar Aïfa, Ibrahima Gassama, Papa Malick Ngom

PII: S1464-343X(18)30141-9
DOI: 10.1016/j.jafrearsci.2018.05.010
Reference: AES 3213
To appear in: *Journal of African Earth Sciences*
Received Date: 20 October 2017
Accepted Date: 23 May 2018

Please cite this article as: Moussa Dabo, Tahar Aïfa, Ibrahima Gassama, Papa Malick Ngom, Revised version Thrust tectonics and transtension tectonics during the Paleoproterozoic evolution of the Birimian Greenstone Belt of Mako, Kédougou-Kéniéba Inlier, Eastern Senegal, *Journal of African Earth Sciences* (2018), doi: 10.1016/j.jafrearsci.2018.05.010

This is a PDF file of an unedited manuscript that has been accepted for publication. As a service to our customers we are providing this early version of the manuscript. The manuscript will undergo copyediting, typesetting, and review of the resulting proof before it is published in its final form. Please note that during the production process errors may be discovered which could affect the content, and all legal disclaimers that apply to the journal pertain.

1
2 **Thrust totranspression and transtension tectonics during the Paleoproterozoic evolution**
3 **of the Birimian Greenstone Belt of Mako, Kédougou-Kéniéba Inlier, Eastern Senegal**

4
5 Moussa Dabo^{1,2}, Tahar Aïfa^{2,*}, Ibrahima Gassama¹, Papa Malick Ngom¹

6
7 ¹Département de Géologie, Faculté des Sciences et Techniques, Université Cheikh Anta Diop de Dakar, BP 5005,
8 Dakar-Fann, Senegal

9 ²Univ Rennes, CNRS, Géosciences Rennes, UMR 6118, 35000 Rennes, France

10 *Corresponding author: tahar.aifa@univ-rennes1.fr
11
12
13
14

15 **Abstract**

16 The structural cartography of the Birimian formations of the Mako area shows a polyphase deformation
17 marked by variable structures such as imbricated shear zones, thrusts and reverse-shears, poly-folding,
18 boudinage, normal faults. The multiscale analysis of the various mapped structures combined with the
19 satellite images allowed us to distinguish three major phases of Eoeburnean and Eburnean deformation.
20 The Eoeburnean D₁ deformation phase is preserved through ductile structures in some lithologies
21 (metabasalts, quartzites). It is composed of early thrusting and late sinistral reverse-shearing due to a
22 NW-SE principal shortening direction, which involved large overturned folds verging northwestward
23 and associated with thrust faults. It is also associated with the emplacement of early granitoids (c. 2200
24 Ma) followed by andesitic to felsic volcanic rocks around c. 2160 Ma. The Eburnean event is divided
25 into two phases of deformation namely D₂ and D₃. The D₂ phase is the early Eburnean event which
26 involves a sinistral transpressive deformation. It is characterized by a NNE-SSW shortening direction
27 which creates major NNW-SSE (N160°-170°) and NNE-SSW (N20°-30) sinistral reverse-shear zones
28 associated with ENE-WSW (N60°-70°) dextral reverse-shear zones. Interference between both major
29 NNE-SSW and NNW-SSE reverse-shear zones involves an anatomizing pattern of deformation. The D₃
30 phase is a transtensional deformation associated with a dextral movement which creates dextral shear
31 zones and conjugate normal faults leading to graben depression. The D₃ principal maximum stress is
32 ENE-WSW oriented. The granitoids were emplaced during these Eoeburnean and Eburnean orogenic
33 events.
34

35 **Keywords:** Eburnean, Birimian, thrust, transpression, transtension, Kédougou-Kéniéba inlier
36
37
38
39
40
41
42
43

1 **1. Introduction**

2 The Man-Leo shield represents the southern part of the West African Craton (WAC). It is composed of
3 two generations of Precambrian rocks, the Paleoproterozoic “Birimian” rocks in the east, and the
4 Archean cratonic nucleus in the west which are tectonically separated by the Sassandra fault (Bessoles,
5 1977; Feybesse et al., 1989; Egal et al., 2002) (Fig. 1a). Birimian terranes of the Kédougou-Kéniéba and
6 Kayes inliers which straddle the border between Senegal and Mali, are the westernmost exposed of the
7 Man-Leo shield (Fig. 1).

8 The Paleoproterozoic “Birimian” terranes of the WAC are formed by sedimentary basins and linear to
9 arcuate volcanic belts intruded by several generations of granitoid plutons. The accretion of these
10 Paleoproterozoic rocks and associated granitoid plutons corresponds to the ‘Eburnean orogeny’ which
11 represent a major juvenile crust-forming event. The term ‘Eburnean’ refers to all tectonic, metamorphic
12 and plutonic events affecting the Birimian rocks during the Paleoproterozoic. The Paleoproterozoic
13 rocks are dated between 2.27 Ga and 2.04 Ga (Bonhomme, 1962 ;Abouchami et al., 1990; Liégeois et
14 al., 1991; Boher et al., 1992; Dia et al., 1992; Davis et al., 1994; Hirdes et al., 1992, 1996; Kouamelan
15 et al., 1997; Doumbia et al., 1998; Gueye et al., 2008; Masurel et al., 2016 ; Parra-Avila et al., 2016 ;
16 Eglinger et al., 2017).

17 A pre-Eburnean cycle in the WAC is suggested by pre-Birimian ages in the time interval of 2266 Ma
18 and 2150 Ma which were obtained on zircon grains from different rocks (sediments, tonalites, granites)
19 of the Man shield (Dia et al., 1992; Davis et al., 1994; Doumbia et al., 1998; Kouamelan et al., 1998;
20 Gueye et al., 2007; Perrouy et al., 2012; Parra-Avila et al., 2016). During this period of time, two
21 orogenic events are distinguished throughout the Birimian with different ages and terminology. In
22 Ghana, the earlier event is referred as the Eoeburnean (2195-2150 Ma) or the Eburnean I (2266-2150
23 Ma) and the latter as the Eburnean (2148-2090 Ma) or the Eburnean II (2216-2088 Ma) (Allibone et al.,
24 2002; de Kock et al., 2011). In Burkina Faso the earlier event is the Tangaeen (2170-2130 Ma) and is
25 followed by the Eburnean (2130-1980 Ma) (Tshibubudze et al., 2009; Hein, 2010).

26 The Eoeburnean to Eburnean orogenies are characterized by a complex tectono-magmatic evolution
27 (Ledru et al., 1989, 1991; Milési et al., 1992; Feybesse et al., 1994; Pons et al. 1994; Vidal et al., 2009;
28 Lompo, 2010; Dabo and Aifa, 2010; Diatta et al., 2017; Masurel et al., 2017). At the scale of the WAC,
29 they are now considered as polycyclic with two models of evolution: (i) the dome and basin geometry
30 model which results of vertical movements due to gravitation instabilities followed by regional-scale
31 transcurrent tectonics (Vidal et al., 2009; Lompo, 2010; Pitra et al., 2010; Delor et al., 2010); (ii) the
32 tangential to transcurrent model with nappes stacking along orogen parallel thrust faults (Ledru et al.,
33 1989; Milési et al., 1992; Feybesse et al., 2006).

34 This paper contributes to the details characterization of the Eoeburnean to Eburnean orogenies in the
35 Mako Greenstone Belt southwestern part of the Kédougou-Kéniéba Inlier (KKI). The goal is to propose
36 a tectonic evolution model based on the analyses of the field structural features. The methodology
37 consists of cartography, detailed structural analysis of field data and satellite images, in order to better
38 constrain the evolution of the Mako Greenstone Belt.

1
2
3
4
5
6
7
8
9
10
11
12
13
14
15
16
17
18
19
20
21
22
23
24
25
26
27
28
29
30
31
32
33
34
35
36
37
38

2. Geological setting

The volcanic, volcano-sedimentary and sedimentary rocks of Paleoproterozoic Birimian of the KKI are arranged into two Supergroups (Bassot, 1987), which are tectonically separated by the SW-NE to NS trends crustal-scale shear zone, the Main Transcurrent Zone (MTZ)(Fig. 1b). The Mako Supergroup to the west is dominantly composed of submarine volcanics, pillowed basalts, andesitic to rhyolitic flows associated with pyroclastites and ultramafic bodies. The volcano-plutonic rocks are bimodal and consist of basal tholeiitic sequence and upper calc-alkaline sequence. The tholeiitic sequence consists of pillowed and massive basalt and ultramafic bodies (Bassot, 1966; Ngom, 1995; Dia et al., 1997; Delor et al., 2010). The mafic and ultramafic assemblages are petrogenetically co-magmatic (Ngom, 1995). They show a tholeiitic affinity relative to mantle plume basalts environment (Abouchami et al 1990; Boher et al., 1992; Pawlig et al., 2006 ; Ngom, et al., 2010; Delor et al., 2010). The emplacement age of the mafic rocks estimated by Sm/Nd method on the whole rock (WR) is 2197 ± 13 Ma (Dia et al., 1992). The ultramafic rocks are not dated yet, however, they are found in inclusions within the mafic rocks and can be regarded as the base of an ophiolitic sequence characteristic of the Birimian formations of the Mako sector (Dabo et al., 2017). It should be noted that previous geochemical, geochronological and lithostratigraphic works (Dia, 1988; Bertrand et al., 1989; Dia et al., 1992) consider the amphibolite-gneisses of Sandikounda-Laminia dated at 2206 ± 6 Ma (Pb/Pb on zircon, Dia et al., 1992) as the base of the Mako Supergroup.

The calc-alkaline rocks are composed of andesitic to rhyolitic flows associated with volcano-sediments (tuffs, pyroclastites, epiclastites) (Ngom, 1995; Dia et al., 1997). They show a geochemical affinity of subduction zones (Delor et al., 2010), and of an Island-arc (Dia, 1988; Pawlig et al., 2006 ; Lambert-Smith et al., 2016). These intermediate and felsic rocks are dated between 2160 ± 16 Ma and 2070 Ma (Calvez et al., 1990; Boher et al., 1992; Hirdes and Davis, 2002). The sedimentary rocks are represented by lenses of quartzites, ribbons of limestones and of conglomerates interstratified within the mafic, intermediate and felsic rocks (Diallo, 1994; Ngom, 1995). The volcano-sediments and sediments represent the top of the lithological sequence of the Mako Supergroup (Dabo et al., 2017).

The Dialé-Daléma Supergroup is dominantly sedimentary (Table 1) and consists of interlayered pelites, sandstones, greywackes, marbles, quartzites and breccias (Milési et al., 1989; Dabo, 2011). It is represented by the upper part of the stratigraphic KKI Birimian formations (Ngom et al., 2010; Delor et al., 2010). Geochronological data from zircons of Dialé-Daléma detrital sedimentary rocks indicate an age between 2093 ± 7 Ma and 2165 ± 1 Ma (Boher et al., 1992; Hirdes and Davis, 2002).

The sedimentary sequence is cross-cut by a calc-alkaline volcanic complex (andesite, rhyodacite, rhyolite) which has orogenic volcanic arc affinities (Milési et al., 1989; Delor et al., 2010; Lambert-Smith et al., 2016). Rhyolitic flow of Daléma has been dated at 2099 ± 4 Ma (Hirdes and Davis, 2002).

Several generations of Eburnean granitoids occurred into the Birimian rocks of the KKI. They form three batholiths: Badon-Kakadian, Saraya and Boboti (Bassot, 1966). Recent works of Théveniaut et al. (2010) regard these batholiths as a suite of granitoids. They distinguish thus three suites of granitoids:

1 Soukouta (former Badon-Kakadian batholith of Bassot (1966)), Saraya and Boboti. The Badon-
2 Kakadian batholith is an assemblage of plutons mainly composed of felsic rocks, dated in the range of
3 2140 Ma to 2213 Ma (Bassot, 1966; Dia, 1988; Dia et al., 1997; Gueye et al., 2008). The Saraya and
4 Boboti batholiths are composed of various granitoids (diorites, granodiorites, granites) with ages ranging
5 between 2100-2060 Ma (Saraya) and 2080-2060 Ma (Boboti) (Bassot, 1966; Hirdes and Davis, 2002;
6 Théveniaut et al., 2010; Lambert-Smith et al., 2016). Recent U-Pb ages data from Boboti and
7 Balangouma plutons in the Boboti batholith, indicate crystallization at 2088.5 ± 8.6 Ma and 2112 ± 13 Ma,
8 respectively and inherited zircons in the the Boboti pluton indicate magmatic activity in the Falémé
9 Belt (Daléma) at 2218 ± 83 Ma (Lambert-Smith et al., 2016; Masurel et al., 2017).

10 The KIBirimirian formations are affected by a regional metamorphism of greenschist facies (Bassot,
11 1966). The amphibolite facies is found in the contact aureole around some granitoid massifs (Bassot,
12 1966; Dia, 1988) and associated with the ultramafic rocks particularly at Lamé sector in the SE of Mako
13 (Dabo et al., 2017). At the scale of the WAC, the greenschist facies metamorphism affected most of the
14 Birimian formations (Debat et al., 2003; Block et al., 2015). It resulted from a large retrograde
15 metamorphism of amphibolite facies which are reworked to greenschist facies (John et al., 1999; Klemm
16 et al., 2002; Block et al., 2015). The greenschist to amphibolite-facies metamorphic assemblages that
17 developed during the Eburnean orogeny are superimposed on an early thermal regime that produced
18 high-pressure greenschist- to blueschist-facies metamorphic assemblages (Ganne et al., 2014).

19 The Eburnean metamorphism is accompanied by deformation whose phases and styles are variously
20 interpreted (Table 2). Some authors (e.g. Leube et al., 1990; Eisenlohr and Hirdes, 1992; Hirdes et al.,
21 1996; Gasquet et al., 2003) argued for a single orogenic cycle. Other authors considered a polycyclic
22 model with two (Ledru et al., 1989), three (Ouedraogo and Prost, 1986; Ouedraogo, 1987; Feybesse et
23 al., 1989, 2006; Milési et al., 1992) or more than three (Block et al., 2015; Baratoux et al., 2015) major
24 phases of Eburnean deformation with variable styles of deformation.

25 1- The first D_1 thrusting phase (Feybesse et al., 1989; Ledru et al., 1989, 1991; Milési et al., 1992) or a
26 peri-plutonic deformation (Pons et al., 1995; Vidal et al., 1996; Debat et al., 2003; Pitra et al., 2010;
27 Delor et al., 2010).

28 2- The second D_2 transcurrent to transpressive phase is responsible for large NS- to NE-trending
29 Eburnean tectonic shear zones and the emplacement of several intrusions within Proterozoic terranes
30 (Ledru et al., 1989, 1991; Liégeois et al., 1991; Pons et al., 1992).

31 3- The third D_3 phase is currently recognized in all the Birimian provinces of the WAC with variable
32 tectonic styles: transcurrent or transtension and/or brittle ductile deformation (Feybesse et al., 1989,
33 2006; Ouedraogo and Prost, 1986; Ouedraogo, 1987; Dabo and Aifa, 2011; Lawrence et al., 2013; Delor
34 et al., 2010).

35 4- The other deformation phases are differently described throughout the WAC according to the
36 Birimian provinces and the authors (Baratoux et al., 2015; Block et al., 2016).

37

38 **3. Lithology of the Mako area**

1 The Mako sector, in the southern part of the Mako Supergroup (Fig. 1b), is primarily made up of
 2 ultramafic, mafic, intermediate and felsic rocks associated with some sedimentary quartzite slices (Fig.
 3 2a). Mafic rocks are most significant and constitute the main part of the greenstone hills between
 4 Sékhoto Peul to the north and Wassadou in the south. Associated with the greenstone mafic hills appear
 5 the Lamé and Massanritana black hills that consist of ultramafic rocks, located at the east and west of
 6 Mako village, respectively. Kilometric lenses of quartzites, NNW-SSE and NE-SW oriented, are
 7 intercalated within the mafic rocks. Breccias and lavas of intermediate and felsic rocks occupy the
 8 tectonic corridors cross-cutting the previous units. Several generations of plutons (granitoids and
 9 gabbros) constitute the main part of the outcrops in Niéméniké village (Fig. 2). The NW-SE cross-section
 10 between Lamé and Sékhoto Peul (Fig. 2b), shows lateral succession of ultramafic rocks, layered
 11 metagabbros, pegmatitic metagabbros and isotropic metagabbros separated by diffuse and irregular
 12 subvertical contacts. In the mylonitic corridor of Bafoundou, the metagabbros are cross-cut by altered
 13 andesitic breccias and pass laterally to quartzites then to metabasalts in pillow lavas. The metabasalts,
 14 often pillowed, are frequent towards Sékhoto Peul. In addition, several generations of plutonic intrusions
 15 (granitoids and gabbros) with variable tectonic fabrics, are emplaced in volcanic and volcano-
 16 sedimentary units between Niéméniké and Sékhoto Peul (Fig. 2).

17 Based on the field geometrical relationship between the different facies, Dabo et al. (2017) distinguished
 18 two lithological units in the Mako area: the tholeiitic ophiolitic complex at the base and the calc-alkaline
 19 mixed volcanic complex at the top, separated by lenses of quartzites (Fig. 3).

20

21 **4. Structural features**

22 The ophiolitic sequence and the mixed volcano-sedimentary complex of the Birimian Greenstone Belt
 23 rocks of Mako (Ngom, 1995; Ngom et al., 2011; Dabo et al., 2017) were subject to polyphase
 24 deformations. These deformations are attributed to Eoeburnean (2195-2150 Ma) and Eburnean (2148-
 25 2060 Ma) events (Bonhomme, 1962; Allibone et al., 2002; Tshibubudze et al., 2009; Hein, 2010; de
 26 Kock et al., 2011). Three phases of deformation are distinguished, they are composed of a major (D_1)
 27 Eoeburnean deformation phase and two (D_2, D_3) major Eburnean deformation phases.

28

29 **4.1. The Eoeburnean D_1 compressive to thrust phase**

30 The Eoeburnean D_1 phase is a compressive deformation which reveals thrust and sinistral reverse-
 31 shearing structures and large overturned folds (Figs. 4;5;6). The thrusts are the early manifestation of
 32 the D_1 phase which ends by sinistral reverse-shearing. The structures of this early deformation phase are
 33 locally preserved in certain rigid lithologies (metaperidotites, metagabbros, metabasalts and ribboned
 34 quartzites) (Figs. 5a-d). The ductile deformation structures are constituted of thrust zones, sinistral
 35 reverse-shearing, folds, L_1 stretching lineation and S_1 foliation (Figs. 4;5;6g,h).

36 The thrust zones and sinistral reverse-shearing are identified and characterized at the scale of the
 37 outcrops (Fig. 5). They mainly show a NE-SW direction which locally varies because of post-
 38 deformation (Eburnean). In the field, the thrust structures are poorly preserved as a result of subsequent
 39 deformation. The thrust planes are marked out by a rough $N40^\circ-45^\circ$ foliation (highlighted by chlorite

1 and sericite minerals) with a variable dip (20° - 30°) towards the SE or the NW (Figs. 5b,c). The stretching
2 lineation (L_1) which accompanies the displacement is hardly identifiable in the metabasalts. However,
3 in the layers of the ribboned quartzites north of Niéméniké, it is slightly underlined by quartz-sericite
4 minerals aggregates stretched in the $N125^{\circ}$ - 25° direction along $N20^{\circ}$ - 20° SE oriented foliation planes
5 (S_1) (Figs. 5c,d).

6 The criteria of displacement associated with these thrusts are shown by the XZ foliation planes by sigma
7 clasts and microfolds which formed at the same time as the foliation and indicate an overlapping towards
8 the NW (Fig. 5d).

9 The sinistral reverse-shearing is responsible for the Massanritana metaperidotites hill displacement by
10 more than 1 km towards the SW (Fig. 2a). The L_1 stretching lineation associated with the displacements
11 is marked by metabasalt enclaves stretching along $N110^{\circ}$ - 70° direction in the Soukourtou granodiorite
12 (Fig. 6h).

13 The folding (P_1) related to this first deformation phase appears at various scales. In the metabasalts, the
14 limbs of the folds (P_1) are highlighted by the inclination and the bending of the pillow axial planes which
15 define a primary bedding (S_0) modeled by a buckled folding of $N60^{\circ}$ - 50° SE axial plane (Figs. 5e,b). In
16 Badian, the interpillow material of the metabasalts shows a P_1 folding (Fig. 6a) which involves high-
17 strain characters. In addition, centimetric P_1 overturned folds are also highlighted by felsic injections
18 within metabasalts. In the metaperidotites, remnants of P_1 folds are locally observed with curvilinear
19 axis (Fig. 6c). On the Aster satellite images, kilometric megafolds, buckled towards the NW, appear on
20 digital terrain models (DTM) in two (2D) and three (3D) dimensions (Fig. 4). These large folds are
21 highlighted by alternation of asymmetric hills and depressions. In the pillow-lava hills, from backlimb
22 to forelimb, the altitude of the main axis dip of pillow bodies indicate asymmetric folding (Figs. 6c,d).
23 Their axes, on average NE-SW oriented, are sometimes upturned by the second post-folding P_2 (Fig. 6b).
24 The principal stress responsible for this Eoeburnean deformation phase would logically be oriented SE-
25 NW taking into consideration conjugate shear joint cross-cutting the pillowed metabasalts body (Figs.
26 6e,f), the asymmetry of P_1 folding (Fig. 5e) as well as criteria of shearing observed in the S_1 foliation
27 planes (Fig. 5d).

28 In addition, the granodiorite of Soukourtou (southern part of the Badon granodiorite) shows ptygmatic
29 overturned folds with $N75^{\circ}$ - 70° SE oriented axial plane, relative to synmagmatic deformation of the D_1
30 phase (Fig. 6g). These folds appear also in the gneiss enclosing the granodiorite and are cross-cut by
31 $N25^{\circ}$ oriented S_2 foliation. This granodiorite contains locally deformed metabasalt enclaves which are
32 often stretched along the $N110^{\circ}$ - 40° L_1 stretching lineation (Fig. 6h). The boundaries between enclaves
33 and granodiorite are sinuous and irregular (contact often in flower structure shape) that attests the
34 contemporaneous emplacements between the two magmatic materials (Fig. 6h). The Badon granitoid is
35 dated around c. 2213 Ma (Bassot and Caen-Vachette, 1984; Gueye et al., 2007), i.e. during the
36 Eoeburnian period.

1 Thus, the D_1 deformation is constrained by the age of emplacement of the early granitoids and
2 metabasalts estimated by Pb/Pb methods on WR and single Zrat 2213 ± 3 Ma and 2195 ± 11 Ma,
3 respectively (Dia, 1988; Gueye et al., 2007).

4 This D_1 deformation would therefore be late to the emplacement of the metabasalts ($\leq c.$ 2195 Ma) and
5 corresponds to the Eoeburnean period. The emplacement of intermediate and felsic volcanic rocks dated
6 at 2160 ± 16 Ma by Sm/Nd on WR (Boher et al., 1992) marks the end of the D_1 Eoeburnean phase.

7 **4.2. The Eburnean D_2 transpressive deformation phase**

8 The D_2 deformation phase is well expressed in the Birimian formation of the Mako area by reverse-shear
9 zones of variable dimensions in which foliation (S_2), lineation (L_2), and folding (P_2) are concentrated
10 and revealed clearly. The semi-ductile and brittle structures (tension gashes, shear joints, rolls, fractures,
11 faults) have a random distribution and are not always located in the shear zones.

12 The reverse-shear zones are oriented according to three conjugate principal directions, NNE-SSW
13 ($N20^\circ-35^\circ$), NNW-SSE ($N160^\circ-170^\circ$) and ENE-WNW ($N60^\circ-70^\circ$) (Figs. 2a,c). A fourth direction, NS
14 oriented, is interpreted to result from local flexure of the path of the NNE-SSW oriented shear zones
15 (Figs. 2a;6e;7a). These shear zones are associated with three major directions of foliation S_{2a} ($N20^\circ-$
16 35°), S_{2b} ($N150^\circ-180^\circ$) and S_{2c} ($N60^\circ-70^\circ$) (Figs. 7b-d). The stretching lineations associated with these
17 various shear zones show a rather moderate to steep plunge ($> 35^\circ$) and a NE-SW to NW-SE and NNW-
18 SSE direction (Fig. 7e).

19 The gentle ENE-WSW ($N60^\circ-70^\circ$) reverse-shear zones, with main S_{2c} $N70^\circ-65$ SSW and minor S_{2a}
20 $N30^\circ-55$ SE foliations, are observed in the andesitic tuffs and ultramafic rocks of the Lamé sector. These
21 shear zones reveal the kinematics criteria of a dextral movement (Fig. 7d) associated with the $N140^\circ-25$
22 oriented mineral stretching lineation. In the Lamé sector the abundance of weathering surface and
23 alluvial deposits often mask these shear zones paths and their contact with the other shear zones (NNE-
24 SSE, NNW-SSE) which were not observed in the field. The most illustrative example of these ENE-
25 WSW dextral reverse-shear zones is the Lamé Shear Zone (LSZ) located in the southeast of Lamé village
26 (Fig. 2a).

27 The reverse-shear zones oriented NNE-SSW are more represented in the north at the Niéméniké sector
28 (Fig. 2a). The NNE-SSW major foliation is associated with a stretching lineation of clasts along with
29 the $N100^\circ-120^\circ$ direction and dip of $25^\circ-60^\circ$ (Fig. 7e). The criteria of rotation in the XY and XZ foliation
30 planes are clasts which indicate a sinistral reverse-shear (Figs. 7e,f).

31 The most important NNW-SSE ($N170^\circ$) shear zone in the study area is that of Bafoundou Corridor (BC)
32 (Fig. 2a). It is a mylonitic corridor which lengthens in the form of depression from the south of the
33 village of Bafoundou until the north of Niéméniké on several kilometers in the NNW-SSE direction
34 (Fig. 2a). Its lateral extension is variable and can reach 3 km locally. The principal foliation $N165^\circ-$
35 50° SW oriented (S_{2b}), crenulates a former foliation (S_{2a}) of $N25^\circ$ to $N30^\circ$ direction with a dip around
36 70° SE (Figs. 7b;8c). The criteria of shearing in the XZ and XY foliation planes (delta clasts, S/C,
37 synfolial folds, etc.) indicate a sinistral reverse-shear (Figs. 7b,c;8c). The stretching lineation in the
38 $N160^\circ$ foliation planes is roughly oriented $N175^\circ-40^\circ$.

1 Throughout this NNW-SSE BC mylonitic corridor most rigid facies (quartzites, metaperidotites)
2 underwent a stretching and a boudinage accompanied by a sinistral shear on their edges (Fig. 2a). They
3 would behave like rigid cores packed in a soft coat represented by the mylonitic facies (breccias, tuffs).
4 Thus, the metaperidotites hill of Massanritana would have undergone at the same time as the ribboned
5 quartzite beds of western Mako, a stretching and a boudinage accompanied by a sinistral shear in the
6 N170° direction. On the vertical plane the conjugate NE-SW and NNW-SSE reverse faults with opposed
7 dips, reveal locally graben structures (Figs. 8c;9a).

8 The P₂ folds related to the Eburnean D₂ compressive phase are mostly of modest size (metric to
9 centimetric). They are often concentrated in the shear zones and sometimes superimposed on the P₁
10 folds. Thus, the gabbros and the rhyolitic tuffs of the BC shear zone show isoclinal folds (P₂) with tilted
11 curved axis oriented N40°-18° and N310°-46°, respectively (Figs. 7e;9b).

12 In addition, on the Aster satellite images, P₂ folding appears by the bending of the P₁ folds axes (Fig. 4).
13 Stereoplot projection of measurements relative to the geometry of the semi-ductile to brittle structures
14 (conjugated joints, slickenside in slip plane) indicate the NNW-SSE direction of the principal maximum
15 stress of this phase (Figs. 6e,f;8b,c). The whole of the structures relevant to D₂ assumes a sinistral
16 transpressive phase with a partitioning of the deformation between the mylonitic zones and the rigid
17 cores which they pack.

18 **4.3. The transtensive D₃ deformation phase**

19 It is a dextral transtensional phase whose deformations are less intense than those of the former phases,
20 primarily marked by semi-ductile and brittle structures. It appears locally by mostly dextral narrow shear
21 zones some of which are related to a reactivation of former sinistral shear zones (Figs. 8d;9e,f). The D₃
22 shear zones are generally oriented NNE-SSW and NNW-SSE with a variable foliation of N20° and
23 N150° direction cross-cutting those of the D₂Eburnean deformation. The stretching lineation associated
24 with this phase is seldom expressed. In the NNE-SSW shear zone affecting the mottled gabbros of
25 Niéméniké, the lineation is underlined by the stretching of the pyroxene needles orualitized along the
26 N25° direction (Fig. 2a). The criteria of the movement observed in these shear zones (extrusion, folds
27 synchronous with foliation development and clasts) reveal a dextral shear (Fig. 9f). However, the relics
28 of a sinistral shear are still perceptible in certain NNE-SSW shear zones (Fig. 9e).

29 In the tuffs of Laméthe NNE-SSW foliation is affected by N160°-60°SE dextral crenulated foliation
30 (Fig. 10a) related to D₂ phase. Also, a crenulated foliation, N160°-60°NW oriented, in a dextral shear
31 appears locally in the pink granite of Niéméniké (Fig. 10b).

32 The semi-ductile deformation is demonstrated by very frequent tension gashes cross-cutting the S₂
33 foliation. In the quartz diorites of Niéméniké and the metabasalts in pillow lavas of western Mako appear
34 tension gashes cross-cutting S₂ indicating a dextral shear. In the light diorite of northern Niéméniké, “en
35 echelon” tension gashes relative to the N70°-60°SE normal fault plane appear locally (Fig. 10c).

36 The brittle deformation appears in the metaperidotites and the tuffs of Mako, marked by a system of
37 conjugate normal faults oriented N140° with opposite dips (NE and SW). They involve the tilt of S₁
38 foliation in the form of drag fold with downthrown side indicating a collapse (Figs. 10d,e). These

1 conjugate normal faults with opposite dips created a graben structure along the Mako village (Figs. 8d;
2 10f). In the north of Niéméniké, the graben structure observed in the silicified metabasalts looks like a
3 negative flower structure (Fig. 10f).

5. Discussion and Conclusions

6 The architecture of the Birimian formations of the KKI is primarily related to the Eoeburnean and
7 Eburnean orogenesis which presents a polyphase evolution at the scale of the WAC (Ledru et al., 1991;
8 Feybesse et al., 2006; Delor et al., 2010; Lompo, 2010; Dabo et al., 2010; Baratoux et al., 2011; Jessell
9 et al., 2012).

10 Our investigations in the Mako area allowed us to distinguish three major phases of Eoeburnean (D_1)
11 and Eburnean (D_2 , D_3) deformations evolving in different tectonic styles (Fig. 8). The D_1 phase is a
12 compressive event which leads to thrust and sinistral reverse-shear zones. It is marked by large
13 overturned folds towards the NW (Figs. 6c,d;8a), relics of thrust and sinistral reverse-shearing associated
14 with stretching lineation generally oriented NW-SE with a variable dip (Fig. 2a). The principal
15 shortening direction associated with this phase of deformation is NW-SE oriented (Figs. 6e,f;8a). These
16 early deformation structures are filled and/or cross-cut by intermediate to acid rocks which are dated
17 around c. 2160 Ma (Boher et al., 1992). The high-strain folding of pillowed metabasalt and pygmatic
18 folding in granodiorite (Fig. 6a,g) suppose a high temperature deformation at the end of the basaltic
19 magma cooling between 2197 ± 13 Ma and 2195 ± 11 Ma using Nd/Sm and Pb/Pb methods on WR,
20 respectively (Bassot et Caen-Vachette, 1984; Dia, 1988; Gueye et al., 2007). Therefore, the D_1
21 deformation phase is believed to have began around c. 2195Ma, after the emplacement of the pillow-
22 lavas basalts. This period of time corresponds to the early Paleoproterozoic event which age and
23 terminology differs throughout the Birimian. In Ghana, the earlier event is referred as Eburnean I (2266-
24 2150 Ma) (Allibone et al., 2002) or as Eoeburnean (2195-2150 Ma) (de Kock et al., 2011). In Burkina
25 Faso, the early Paleoproterozoic event is the Tangean which corresponds to the period between 2170
26 Ma and 2130 Ma (Tshibubudze et al., 2009; Hein, 2010). In the Birimian of the KKI, Delor et al. (2010)
27 revealed an early Eburnean phase of gravity deformation (D_g) related to Eoeburnean diapirism
28 associated with the plutonism of the Sandikounda-Soukouta Suites.

29 Our interpretation is that in the Mako area of KKI, the early Eoeburnean deformation (D_1), characterized
30 by thrust to sinistral reverse-shear deformation is associated with large overturned folds and a regional
31 NNW-SSE shortening that occurred at approximately 2.19-2.17Ga.

32 An early Eburnean compressive to thrust deformation, i.e. D_1 deformation phase, was announced in the
33 sedimentary Birimian formations of the Dialé-Daléma Supergroup (Ledru et al., 1989; Milési et al.,
34 1992; Dabo and Aïfa, 2010). The age of this early Eburnean deformation is not specified in this
35 Supergroup.

36 In the Birimian formations of Ghana, a D_1 -thrust deformation with SW vergence (Feybesse et al., 2006)
37 associated with reverse shear zone and large scale folds (Block et al., 2016), similar to those of Mako,
38 is reported in the D_1 Eburnean phase.

1 The Eoeburnean event has variably characteristics through the WAC. In Ghana, it reveals the
2 development of regional scale folds and bedding parallel foliation, associated with the development of
3 east-west trending structures during a regional north-south shortening (Perrouy et al., 2012). In Burkina
4 Faso, the Tangaeen event (2170-2130 Ma) is characterized by northwest to north-northwest trending
5 dextral-reverse shear zones, and fold-thrust belts that developed during a period of northeast-southwest
6 crustal shortening (Tshibubudze et al., 2009 ; Hein, 2010).

7 The late stage of the D₁ deformation phase is marked by the emplacement of intermediate and felsic
8 volcanic rocks which are dated around c. 2160 Ma (Boher et al., 1992).

9 In NW of Ghana, the N-S extensional deformation followed the D₁ Eburnean phase (Block et al., 2016).
10 According to Feybesse et al. (2006), this period of extensional tectonic precedes or was partly
11 contemporaneous with the first Eburnean deformation phase in Ghana.

12 The structures of the Eoeburnean phase are generally disturbed and overturned by the Eburnean
13 deformations (Fig. 8b). The Eburnean D₂ phase of deformation is a transpressive tectonics which
14 revealed sinistral NNE-SSW and NNW-SSE, and dextral ENE-WSW conjugate reverse-shear zones
15 (Fig. 8c'). These NNW-SSE and NNW-SSE shears may have played the part of R and P structures in a
16 NS oriented Riedel system where ENE-SSW shears represent the R' structures (Fig. 8c').

17 The principal shortening is NNW-SSE oriented according to brittle structures geometries (Figs. 9c,d;
18 8d'). In the course of the deformation the NNW-SSE oriented sinistral reverse-shear zones which cross-
19 cut the preceding ones (NNE-SSW), involve a flexure of their ends according to a N-S direction (Fig.
20 7a).

21 The anastomosed interconnection of very deformed shear zones (NNE-SSW and NNW-SSE) which
22 frame the cores of little-deformed rocks results in the deformation partitioning.

23 This Eburnean D₂ phase is similar to those described in the Dialé-Daléma Supergroup (Ledru et al.,
24 1989; Dabo et al., 2010) as well as in the Birimian of Burkina Faso (Baratoux et al., 2015; Tshibubudze
25 et al., 2015) and Ghana (Feybesse et al., 2006).

26 Throughout the WAC the age of the early Eburnean deformation phase (denoted here D₂) is estimated
27 between 2140 Ma and 2100 Ma contemporaneously with the emplacement of the syntectonic Eburnean
28 granitoids dated between c. 2142 Ma and c. 2102 Ma (Bassot and Caen-Vachette, 1984; Liégeois et al.,
29 1991; Dia et al., 1997; Hirdes and Davis, 2002; Gueye et al., 2007; Delor et al., 2010; Goujou et al.,
30 2010; Block et al., 2015; Lambert-Smith et al., 2016).

31 The Eburnean D₃ phase is a dextral transtension mainly with semi-ductile and brittle structures. It is
32 characterized by narrow shear zones NNE-SSW and NNW-SSE oriented with dextral movement. Some
33 of these shear zones could result from a reactivation of D₂ sinistral reverse-shear zones (Figs. 9e,f). The
34 other structures of this phase are the graben structures which result from a set of conjugate normal faults
35 (Figs. 10d-f). The principal shortening responsible for these deformations is inferred to be oriented
36 NNE-SSW (Figs. 9c,d). All these Eburnean structures of the D₃ deformation phase indicate a less intense
37 deformation than those of the Eburnean D₁ and D₂ deformation phases and characterize a dextral
38 transtension.

1 The Eburnean D₃ deformation probably occurred between 2100 Ma and 2060 Ma associated with the
 2 emplacement of the syntectonic granitoids of Saraya and Boboti Suite which are dated between 2100
 3 Ma and 2060 Ma (Abouchami et al., 1990; Hirdes and Davis, 2002; Gueye et al., 2007; Delor et al.,
 4 2010).

5 In the Dialé-Daléma Supergroup, the D₃ Eburnean deformation characterized by different structures
 6 with local reactivation of old D₂ sinistral shear zones (Delor et al., 2010; Dabo and Aïfa, 2011; Lawrence
 7 et al., 2013). At the scale of the KKI, Delor et al. (2010) distinguished an Eburnean D₃ transcurrent phase
 8 (Dt₃) characterized by conjugate zones of NE-SW dextral and NW-SE sinistral shears.

9 In the other Birimian provinces of the WAC, the Eburnean D₃ phase is also less intense than the former
 10 Eburnean phases (Feybesse et al., 2006; Lompo, 2010; Baratoux et al., 2011). In Ghana, it involves
 11 major ENE-SSW to minor WNW- ESE dextral shear zones with a local reactivation into dextral of the
 12 old NE-SW sinistral shear zones (Feybesse et al., 2006). In Burkina Faso, it is marked either by thrusts
 13 with northern or southern dip and an E-W crenulation foliation associated with kink folds (Baratoux et
 14 al., 2011) or by a transtension with dominant NE-SW dextral shear faults (Lompo, 2010).

15 Thus, the Mako sector in line with many Birimian provinces of the WAC is marked by a polyphase
 16 Eoeburnean to Eburnean deformations. The Eoeburnean began with compression which leads to thrusts
 17 towards the southwest associated with a sinistral reverse shearing (D₁) and subsequently the
 18 emplacement of intermediate to felsic volcanic rocks at around c. 2.16 Ga. The Eburnean event is marked
 19 by a sinistral transpression with NNE-SSW shortening direction (D₂) followed by dextral transtension
 20 with ENE-WSW shortening direction (D₃).

21 Plutonic intrusions emplaced before and during the Eburnean deformation phases, i.e. between 2213 Ma
 22 and 2060 Ma (Abouchami et al., 1990; Dia et al., 1992; Hirdes and Davis, 2002; Gueye et al., 2007;
 23 Delor et al., 2010). The metamorphism evolves from greenschist to amphibolite facies (Bassot, 1966,
 24 Dia et al., 1992; Delor et al., 2010; Dabo et al., 2017).

25

26 Acknowledgments

27 This paper benefited from careful and constructive comments from L. Baratoux, N. Thébaud and an
 28 anonymous referee. This is an IGCP638 contribution.

29

30 References

- 31 Abouchami, V., Boher, M., Michard, A., Albarède, F.N.T., 1990. A Major 2.1 Ga old event of mafic
 32 magmatism in West Africa: an early stage of crustal accretion. *Geophysical Research Letters*, 95,
 33 17605-17629.
- 34 Allibone, A., McCuaig, C.T., Harris, D., Etheridge, M., Munroe, S., Byrne, D., Amanor, J., Gyapong,
 35 W., 2002. Structural controls on gold mineralization at the Ashanti gold deposit, Obuasi, Ghana.
 36 *Soc. Econ. Geol. Special Publ.*, 9, 65-93.
- 37 Baratoux, L., Metelka, V., Naba, S., Jessell, M.W., Grégoire, M., Ganne, J., 2011. Juvenile
 38 Paleoproterozoic crust evolution during the Eburnean orogeny (~2.2-2.0 Ga), western Burkina Faso.
 39 *Precambrian Research*, 191, 18-45.

- 1 Bassot, J.P., 1966. Etude géologique du Sénégal oriental et de ses confins guinéo-maliens. *Mémoires*
2 *B.R.G.M.*, 40, 1-332.
- 3 Bassot, J.P., 1987. Le complexe volcano-plutonique calco-alkalin de la rivière Daléma (Est Sénégal):
4 discussion de sa signification géodynamique dans le cadre de l'orogénie éburnéenne (Protérozoïque
5 inférieur). *Journal of African Earth Sciences*, 6 (1), 109-115.
- 6 Bassot, J.P., Caen-Vachette, M., 1984. Données géochronologiques et géochimiques nouvelles sur les
7 granitoïdes de l'Est Sénégal: implication sur l'histoire géologique du Birrimien de cette région.
8 *In: Géologie Africaine*, Tervuren, J. Klerkx and J. Michot (Eds.), 1991-209.
- 9 Bassot, J.P., Dommanget, A., 1986. Mise en évidence d'un accident majeur affectant le
10 Paléoprotérozoïque inférieur des confins sénégal-maliens. *Comptes Rendus Académie des*
11 *Sciences*, Paris, 302, 1101-1106.
- 12 Bertrand, J.M., Dia, A., Dioh, E., Bassot, J.P., 1989. Réflexions sur la structure interne du Craton Ouest
13 africain au Sénégal oriental et confins guinéo-maliens. *Comptes Rendus Geoscience*, Paris, 309,
14 II, 751-756.
- 15 Bessoles, B., 1977. Géologie de l'Afrique. Le craton Ouest-Africain. *Mémoires BRGM*, Paris, 88p.
- 16 Block, S., Ganne, J., Baratoux, L., Zeh, A., Parra-Avila, L.A., Jessell, M., Ailleres, L., Siebenaller, L.,
17 2015. Petrological and geochronological constraints on lower crust exhumation during
18 Paleoproterozoic (Eburnean) orogeny, NW Ghana, West African Craton. *Journal of*
19 *metamorphic Geology*, 33, 463-494.
- 20 Boher, M., 1991. Croissance crustale en Afrique de l'Ouest à 2,1 Ga. Apport de la géochimie isotopique.
21 *Thèse Université de Nancy I*, France, 180p.
- 22 Boher, M., Abouchami, W., Michard, A., Albarède, F., Arndt, N., 1992. Crustal growth in West-Africa
23 at 2.1 Ga. *Journal of Geophysical Research*, 97, 345-369.
- 24 Bonhomme, M., 1962. Contribution à l'étude géochronologique de la plate-forme de l'Ouest Africain.
25 *Annales de la Faculté des Sciences de l'Université de Clermont-Ferrand. Geol. Miner.*, 5, 62.
- 26 Dabo, M., Aïfa, T., 2010. Structural Styles and Tectonic evolution of the Kolia-Boboti sedimentary
27 basin, Kédougou-Kéniéba inlier, eastern Senegal. *Comptes Rendus Geoscience*, 342, 796-805.
- 28 Dabo, M., Aïfa, T., 2011. Late Eburnean deformation in the Kolia-Boboti sedimentary basin, Kédougou-
29 Kéniéba inlier, Sénégal. *Journal of African Earth Sciences*, 60, 106-116.
- 30 Dabo, M., Aïfa, T., Gning, I., Faye, M., Ba, M.F., Ngom, P.M., 2017. Lithological Architecture and
31 Petrography of the Mako Birimian Greenstone Belt, Kédougou-Kéniéba Inlier, Eastern Senegal.
32 *Journal of African Earth Sciences*, 131, 128-144.
- 33 Davis, D.W., Hirdes, W., Schaltegger, E., Nunoo, E.A., 1994. U/Pb age constraints on deposition and
34 provenance of Birimian and gold-bearing Tarkwaian sediments in Ghana, West Africa. *Precambrian*
35 *Research*, 67, 89-107.
- 36 deKock, G.S., Theveniaut, H., Botha, P.M.W., Gyapong, W., 2012. Timing the structural events in the
37 Palaeoproterozoic Bole-Nangodi belt terrane and adjacent Maluwe basin, West African Craton, in
38 central-west Ghana. *Journal of African Earth Sciences*, 65, 1-24.
- 39 Debat, P., Nikiéma, S., Mercier, A., Lompo, M., Béziat, D., Bourges, F., Roddaz, M., Salvi, S., Tollon,
40 F., Wenmenga, U., 2003. A new metamorphic constraint for the Eburnean orogeny from
41 Palaeoproterozoic formations of the Man shield (Aribinda and Tampilga countries, Burkina Faso).
42 *Precambrian Research*, 123, 47-65.
- 43 Delor, C., Couëffé, R., Goujou, J.C., Diallo, D.P., Théveniaut, H., Fullgraf, T., Ndiaye, P.M., Dioh, E.,
44 Blein O., Barry, T.M.M., Cocherie, A., Le Métour, J., Martelet, G., Sergeev, S., Wemmer, K.,
45 2010. Notice explicative de la carte géologique à 1/200 000 du Sénégal, feuille Saraya-Kédougou
46 Est. Ministère des Mines, de l'Industrie, de l'Agro-Industrie et des PME, *Direction des Mines et de*
47 *la Géologie*, Dakar.
- 48 Dia, A., 1988. Caractère et signification des complexes magmatiques et métamorphiques du secteur de
49 Sandikounda-Laminia (Nord de la boutonnière de Kédougou, Est du Sénégal): un modèle

- 1 géodynamique du Birimien de l'Afrique de l'Ouest. *Thèse Université Cheikh Anta Diop, Dakar*,
2 Sénégal, 350p.
- 3 Dia, A., van Schmus, W.R., Kröner, A., 1997. Isotopic constraints on the age and formation of a
4 Palaeoproterozoic volcanic arc complex in the Kedougou inlier, eastern Senegal, West Africa.
5 *Journal of African Earth Sciences*, 24 (3), 197-213.
- 6 Diallo, D.P., 1994. Caractérisation, d'une portion de croûte d'âge protérozoïque inférieur du craton ouest
7 africain: Cas de l'encaissant des granitoïdes dans le Supergroupe de Mako (boutonnière de
8 Kédougou) - implications géodynamiques. *Thèse Université Cheikh Anta Diop, Dakar*, Sénégal,
9 466p.
- 10 Diallo, D.P., Debat, P., Rocci, G., Dia, A., Ngom, P.M., Sylla, M., 1993. Pétrographie et géochimie des
11 roches méta-volcano-detritiques et méta-sédimentaires du Protérozoïque inférieur du Sénégal
12 oriental dans le Supergroupe de Mako (Sénégal, Afrique de l'Ouest): incidences géotectoniques.
13 *Publications Occasionnelles CIFEG*, 23, 1115.
- 14 Diatta, F., Ndiaye, P.M., Diène, M., Amponsah, P.O., Ganne, J., 2017. The structural evolution of the
15 Dialé-Daléma basin, Kédougou-Kéniéba Inlier, eastern Sénégal. *Journal of African Earth Sciences*,
16 129, 923-933.
- 17 Dommanget, A., Milési, J.P., Diallo, M., 1993. The Loulo gold and tourmaline-bearing deposit: a
18 polymorph type in the early Proterozoic of Mali (West Africa). *Mineral. Deposita*, 28, 253-263.
- 19 Dombia, S., Pouclet, A., Kouamelan, A., Peucat, J.P., Vidal, M., Delor, C., 1998. Petrogenesis of
20 juvenile-type Birimian (Paleoproterozoic) granitoids in Central Côte-d'Ivoire, West-Africa:
21 geochemistry and geochronology. *Precambrian Research*, 87, 33-63.
- 22 Egal, E., Thiéblemont, D., Lahondère, D., Guerrot, C., Costea, C.A., Iliescu, D., Delor, C., Goujou, J.C.,
23 Lafon, J.M., Tegye, M., 2002. Late Eburnean granitization and tectonics along the western and
24 northwestern margin of the Archean Kenema- Man domain (Guinea West African Craton).
25 *Precambrian Research*, 117, 57-84.
- 26 Eglinger, A., Thébaud, N., Zeh, A., Davis, J., Miller, J., Parra-Avila, L.A. Loucks, R., McCuaig, C.,
27 Belousova, E., 2017. New insights into the crustal growth of the Paleoproterozoic margin of the
28 Archean Kéména-Man domain, West African craton (Guinea): Implications for gold mineral
29 system. *Precambrian Research*, 292, 258-289
- 30 Eisenlohr, B.N., Hirdes, W., 1992. The structural development of the early Proterozoic Birimian and
31 Tarkwaian rocks of southwest Ghana, West Africa. *Journal of African Earth Sciences*, 14, 313-325.
- 32 Feybesse, J.L., Billa, M., Guerrot, C., Duguey, E., Lescuyer, J.L., Milesi, J.P., Bouchot, V., 2006. The
33 paleoproterozoic Ghanaian province: Geodynamic model and ore controls, including regional stress
34 modeling. *Precambrian Research*, 149, 149-196.
- 35 Feybesse, J.L., Milési, J.P., Johan, V., Dommanget, A., Calvez, J.Y., Boher, M., Abouchami, W., 1989.
36 La limite Archéen-Protérozoïque inférieur de l'Afrique de l'Ouest: une zone de chevauchement
37 majeur antérieure à l'accident de Sanssandra: l'exemple des régions d'Odienné et de Touba (Côte
38 d'Ivoire). *Comptes Rendus Académie des Sciences*, Paris, 309, 1847-1853.
- 39 Ganne, J., Gerbault, M., Block, 2014. Thermo-mechanical modelling of lower crust exhumation-
40 constraints from the metamorphic record of the Palaeoproterozoic Eburnean orogeny, West African
41 Craton. *Precambrian Research*, 243, 88-109.
- 42 Gasquet, D., Barbey, P., Adou, M., Paquette, J.L., 2003. Structure Sr-Nd isotope geochemistry and
43 zircon U-Pb geochronology of the granitoids of the Dabakala area (Cote d'Ivoire): evidence for a 2.3
44 Ga crustal growth event in the Palaeoproterozoic of West Africa. *Precambrian Research*, 127, 329-
45 354.
- 46 Goujou, J.C., Buscail, F., Théveniaut, H., Dioh, E., Delor, C., Blein, O., Diallo, D.P., Ndiaye, P.M., Le
47 Métour, J., Fullgraf, T., Caby, R., Couëffé, R., Martelet, G., Sergeev, S., Tegye, M., Villeneuve,
48 M., Wemmer, K., 2010. Notice explicative de la cartogéologique à 1/200 000 du Sénégal, feuille
49 Kossanto-Dalafi Est, 2010, Ministère des Mines, de l'Industrie, de l'Agro-Industrie et des PME.
50 *Direction des Mines et de la Géologie*, Dakar.

- 1 Gueye, M., Ngom P.M., Diène M., Thiam Y., Siegesmund S., Wemmer K., Pawlig S., 2008. Intrusive
2 rocks tectono-metamorphic evolution of the Mako Paleoproterozoic belt (Eastern Senegal, West
3 Africa). *Journal of African Earth Sciences*, 50, 88-110.
- 4 Gueye, M., Siegesmund, S., Wemmer, K., Pawlig, S., Drobe, M., Nolte, N., Layer, P., 2007. New
5 evidences for an early Birimian evolution in the West African Craton: An example from the
6 Kédougou-Kéniéba Inlier, Southeast Sénégal. *South African Journal of Geology*, 110, 511-534.
- 7 Hein, K.A.A., 2010. Succession of structural events in the Goren greenstone belt (Burkina Faso):
8 implications for West African tectonics. *Journal of African Earth Sciences*, 56, 83-94.
- 9 Hirdes, W., Davis, D.W., 2002. U/Pb Geochronology of Paleoproterozoic rocks in the Southern part of
10 the Kedougou-Kéniéba inlier, Senegal, West Africa: evidence for diachronous accretionary
11 development of the eburnean province. *Precambrian Research*, 118, 83-99.
- 12 Hirdes, W., Davis, D.W., Eisenlohr, B.N., 1992. Reassessment of Proterozoic granitoid ages in Ghana
13 on the basis of U/Pb zircon and monazite dating. *Precambrian Research*, 56, 89-96.
- 14 Hirdes, W., Davis, D.W., Ludtke, G., Konan, G., 1996. Two generations of Birimian (Paleoproterozoic)
15 volcanic belts in northeastern Cote d'Ivoire (West Africa): consequences for the 'Birimian
16 controversy. *Precambrian Research*, 80, 173-191.
- 17 Jessell, M.W., Amponsah, P.O., Baratoux, L., Asied, D.K., Loh, G.K., Ganne, J., 2012. Crustal-scale
18 transcurrent shearing in the Paleoproterozoic Sefwi-Sunyani-Comoé region, West Africa.
19 *Precambrian Research*, 212-213, 155-168.
- 20 John, T., Klemd, R., Hirdes, W., Loh, G., 1999. The metamorphic evolution of the Paleoproterozoic
21 (Birimian) volcanic Ashanti belt (Ghana, West Africa). *Precambrian Research*, 98, 11-30.
- 22 Kitson, A.E., 1928. Provisional geological map of the Gold Coast and western Togoland with brief
23 descriptive notes. *Gold Coast Geology Survey Bulletin*, 2, 13p.
- 24 Klemd, R., Hünken, U., Olesch, M., 2002. Metamorphism of the country rocks hosting gold-sulfide
25 bearing quartz veins in the Paleoproterozoic southern Kibi-Winneba belt (southeast-Ghana).
26 *Journal of African Earth Sciences*, 35, 199-211.
- 27 Kouamelan, A.N., Peucat, J.J., Delor, C., 1997. Reliques archéennes (3,15 Ga) au sein du magmatisme
28 birimien (2,1 Ga) de Côte d'Ivoire, craton ouest-africain. *Comptes Rendus Académie des Sciences*,
29 Paris, 324 (IIa), 719-727.
- 30 Lambert-Smith, J.S., Lawrence, D.M., Müller, W., Treloar, P.J., 2016. Palaeotectonic setting of the
31 south-eastern Kédougou-Kéniéba Inlier, West Africa: New insights from igneous trace element
32 geochemistry and U-Pb zircon ages. *Precambrian Research*, 274, 110-135.
- 33 Lawrence, D.M., Treloar, P.J., Rankin, A.H., Harbidge, P., Holliday, J., 2013. The geology and
34 mineralogy of the Loulo mining district, Mali, West Africa: Evidence for two distinct styles of
35 orogenic gold mineralization. *Economic Geology*, 108, 199-227.
- 36 Ledru, P., Milési, J.P., Vinchon, C., Ankrah, P., Johan, V., Marcoux, E., 1988. Geology of the Birimian
37 series of Ghana. In: Abstr. Int. Conf. and Workshop on the Geology and Exploration in Ghana and
38 in selected other Precambrian Terrains. 75th Anniversary, *Ghana Geology Survey Department*,
39 Accra Ghana, 26-27.
- 40 Ledru, P., Pons, J., Feybesse, J.L., Dommagnet, A., Johan, V., Diallo, M., Vinchon, C., 1989. Tectonique
41 transcurrente et évolution polycyclique dans le Birimien, Protérozoïque inférieur du Sénégal-Mali
42 (Afrique de l'Ouest). *Comptes Rendus Académie des Sciences*, Paris, 308, 117-122.
- 43 Ledru, P., Pons, J., Milési, J.P., Feybesse, J.L., Johan, V., 1991. Transcurrent tectonics and polycyclic
44 evolution in the lower Proterozoic of Senegal-Mali. *Precambrian Research*, 50, 337-354.
- 45 Lemoine, S., 1982. Le décrochement ductile de Brobo, un linéament éburnéen majeur, son rôle possible
46 dans l'orogène éburnéenne en Côte d'Ivoire. *Comptes Rendus Académie des Sciences*, Paris,
47 295(2), 601-606.
- 48 Lemoine, S., 1988. Evolution géologique de la région de Dabakala (NE de la Côte d'Ivoire) au
49 Protérozoïque inférieur. Possibilité d'extension au reste de la Côte d'Ivoire et au Burkina Faso:

- 1 similitudes et différences: les linéaments greenville-Ferkessédougou et Grand Cess-
2 Niakaramandougou. *Thèse d'état, Université de Clermont-Ferrand, France*, 388p.
- 3 Leube, A., Hirdes, W., Mauer, R., Kesse, G.O., 1990. The early Proterozoic Birimian Supergroup of
4 Ghana and some aspects of its associated gold mineralization. *Precambrian Research*, 46, 139-
5 165.
- 6 Liégeois, J.P., Claessens, W., Camara, D., Klerkx, J., 1991. Short-lived Eburnian orogeny in South Mali.
7 Geology, tectonics, U-Pb&Rb-Sr geochronology. *Precambrian Research*, 50, 111-136.
- 8 Lompo, M., 2010. Paleoproterozoic structural evolution of the Man-Leo Shield (West Africa). Key
9 structures for vertical to transcurrent tectonics. *Journal of African Earth Sciences*, 58, 19-36.
- 10 Lüdtke, G., Hirdes, W., Konan, G., Koné, Y., Yao, C., Diarra, S., Zamblé, Z., 1998. Géologie de la
11 région Haute Comoé Nord-feuilles Kong (4b et 4d) et Téhini-Bouna (3a à 3d). *Direction de la*
12 *Géologie Abidjan Bulletin*, 178p.
- 13 Masurel, Q., Miller, J., Hein, K.A.A., Hanssen, E., Thébaud, N., Ulrich, S., Kaisin, J., Tessougue, S.,
14 2016. The Yatela gold deposit in Mali, West Africa: The final product of a long-lived history of
15 hydrothermal alteration and weathering. *Journal of African Earth Sciences*, 113, 73-87.
- 16 Masurel, Q., Thébaud, N., Miller, J., Ulrich, S., 2017. The tectono-magmatic framework to gold
17 mineralisation in the Sadiola-Yatela gold camp and implications for the paleotectonic setting of the
18 Kédougou-Kéniéba inlier, West Africa. *Precambrian Research*, 292, 35-56.
- 19 Milési, J.P., Ledru, P., Feybesse, J.L., Dommanget, A., Marcoux, E., 1992. Early Proterozoic ore deposits
20 and tectonics of the Birimian orogenic belt, West Africa. *Precambrian Research*, 58, 305-344.
- 21 Milési, J.P., Diallo, M., Feybesse, J.L., Keita, F., Ledru, P., Vinchon, C., Dommanget, A., 1986.
22 Caractérisation lithostructurale de deux ensembles successifs dans les séries birimiennes de la
23 boutonnière de Kédougou (Mali-Sénégal) et du Niandan (Guinée); implications gíafilogéniques.
24 *Publication CIFEG*, 1986/10, les formations birimiennes de l'Afrique de l'Ouest, 113-121.
- 25 Milési, J.P., Feybesse, J.L., Ledru, P., Dommanget, A., Quedraogo, M.F., Marcoux, E., Prost, A.,
26 Vinchon, C., Sylvain, J.P., Johan, V., Tegye, M., Calvez, J.Y., Lagny, P., 1989. Les minéralisations
27 aurifères de l'Afrique de l'Ouest. Leurs relations avec l'évolution lithostructurale au Protérozoïque
28 inférieur. *Chronique Recherche Minière*, 497, 3-98.
- 29 Ngom, P.M., 1989. Caractères géochimiques des formations Birimiennes du supergroupe de Mako
30 (Sabodala et ses environs). *Journal of African Earth Sciences*, 8, 91-97.
- 31 Ngom, P.M., 1995. Caractérisation de la croûte birimienne dans les parties centrale et méridionale du
32 Supergroupe de Mako. Implications géochimiques et pétrogénétiques. *Thèse de Doctorat d'Etat,*
33 *Université Cheikh Anta Diop, Dakar, Sénégal*, 240p.
- 34 Ngom, P.M., Cissokho, S., Gueye, M., Joron, J.L., 2011. Diversité du volcanisme et évolution
35 géodynamique au Paléoprotérozoïque: exemple du Birimien de la boutonnière de Kédougou-
36 Kéniéba (Sénégal). *Africa Geoscience Review*, 18(1), 1-22.
- 37 Ngom, P.M., Cordani, U.G., Teixeira, W., Janasi, V.D.A., 2010. Sr and Nd isotopic geochemistry of the
38 early ultramafic-mafic rocks of the Mako bimodal volcanic belt of the Kedougou-Kenieba inlier
39 (Senegal). *Arabian Journal of Geosciences*, 3, 49-57.
- 40 Ouedraogo, M.F., 1987. Cartographie minérale et implications métallogéniques au Burkina-Faso. *Thèse*
41 *de doctorat 3^e cycle*, Université d'Orléans, France, 234p.
- 42 Ouedraogo, M.F., Prost, A.E., 1986. Mise en évidence des relations entre schistosités et plissements
43 dans la ceinture volcanique birimienne de Yako-Batié (Burkina Faso). *Comptes Rendus Académie*
44 *des Sciences*, Paris, 303(2), 19, 1713-1718.
- 45 Parra-Avila, L.A., Belousova, E., Fiorentini, M.L., Baratoux, L., Davis, J., Miller, J., McCuaig, T.C.,
46 2016. Crustal evolution of the Paleoproterozoic Birimian terranes of the Baoulé-Mossi domain,
47 southern West African Craton: U-Pb and Hf-isotope studies of detrital zircons. *Precambrian*
48 *Research*, 274, 25-60.

- 1 Perrouty, S., Aillères, L., Jessell, M.W., Baratoux, L., Bourassa, Y., Crawford, B., 2012. Revised
 2 Eburnean geodynamic evolution of the gold-rich southern Ashanti Belt, Ghana, with new field and
 3 geophysical evidence of pre-Tarkwaian deformations. *Precambrian Research*, 204, 12-39.
- 4 Pitra, P., Kouamelan, A.N., Ballèvre, M., Peucat, J.J., 2010. Palaeoproterozoic high-pressure granulite
 5 overprint of the Archean continental crust: evidence for homogeneous crustal thickening (Man Rise,
 6 Ivory Coast). *Journal of Metamorphic Geology*, 28, 41-50.
- 7 Pons, J., Barbey, P., Dupuis, D., Léger, J.M., 1995. Mechanism of pluton emplacement and structural
 8 evolution of 2.1Ga juvenile continental crust: the Birimian of south-western Niger. *Precambrian
 9 Research*, 70, 281-301.
- 10 Pons, J., Oudin, C., Valéro, J., 1992. Kinematics of large syn-orogenic intrusions: example of the lower
 11 Proterozoic Saraya batholith (eastern Senegal). *Geologische Rundschau*, 81 (2), 473-486.
- 12 Pouclet, A., Doumbia, S., Vidal, M., 2006. Geodynamic setting of Birimian volcanism in central Ivory
 13 Coast (western Africa) and its place in the Paleoproterozoic evolution of the man Shield. *Bulletin
 14 de la Société géologique de France*, 177(2), 105-121.
- 15 Pouclet, A., Vidal, M., Delor, C., Simeon, Y., Alric, G., 1996. Le volcanisme birimien du nord-est de la
 16 Côte d'Ivoire, mise en évidence de deux phases volcano-tectoniques distinctes dans l'évolution
 17 géodynamique du Paléoprotérozoïque. *Bulletin de la Société géologique de France*, 167 (4), 529-
 18 541.
- 19 Théveniaut, H., Ndiaye, P.M., Buscail, F., Couëffé, R., Delor, C., Fullgraf, T., Goujou, J.C., 2010.
 20 *Notice explicative de la carte géologique du Sénégal oriental à 1/500 000*. Ministère des Mines, de
 21 l'Industrie, de l'Agro-Industrie et des PME, *Direction des Mines et de la Géologie*, Dakar, 120p.
- 22 Tshibubudze, A., Hein, K.A.A., Marquis, P., 2009. The Markoye shear zone in NE Burkina Faso.
 23 *Journal of African Earth Sciences*, 55, 245-256.
- 24 Tshibubudze, A., Hein, K.A.A., McCuaig, T.C., 2015. The relative and absolute chronology of strato-
 25 tectonic events in the Gorom-Gorom granitoid terrane and Oudalan-Gorouol belt, northeast Burkina
 26 Faso. *Journal of African Earth Sciences*, 112, 382-418.
- 27 Vidal, M., Delor, C., Pouclet, A., Siméon, Y., Alric, G., 1996. Evolution géodynamique de l'Afrique de
 28 l'Ouest entre 2,2 Ga et 2 Ga: le style "archéen" des ceintures vertes et des ensembles sédimentaires
 29 birimiens du nord-est de la Côte d'Ivoire. *Bulletin de la Société géologique de France*, 167(3), 307-
 30 319.
- 31 Vidal, M., Gumiaux, C., Cagnard, F., Pouclet, A., Ouattara, G., Pichon, M., 2009. Evolution of a
 32 Paleoproterozoic "weak type" orogeny in the West African Craton (Ivory Coast). *Tectonophysics*,
 33 477, 145-159.

35 Tables Captions

36 Table 1: Lithostratigraphy of the Birimian formations of KKI from bottom to top

37 Table 2: Eoeburnean and Eburnean deformation phases in some Birimian provinces of the WAC

39 Figures captions

40 **Figure 1:** Kédougou-Kéniéba Inlier (KKI) in the Man shield, southern part of the West African Craton
 41 (WAC). (a) Schematic map of the major Precambrian greenstone belts of the southern part of the
 42 WAC (simplified from Pouclet et al., 2006). (b) Simplified geological map of the Birimian of KKI
 43 (modified after Pons et al., 1992). Rectangle delimits the study area. Bo: Boboti; Gm: Gamaye;
 44 MTZ: Main Transcurrent Zone; SMF: Senegalo-Malian Fault.

45 **Figure 2:** (a) Geological map of the Mako Paleoproterozoic Greenstone Belt (modified after Dabo et al.,
 46 2017): BC: Bafoundou Corridor; LSZ: Lamé Shear Zone; MSZ: Mako Shear Zone. (b) Geological

1 sections (AA') showing the geometrical relations between different lithologies (the vertical scale is
 2 approximative). (c) Equal area projection, lower hemisphere, showing foliation and shear planes
 3 orientations in the study area. RN7: trunk road n°7.

4 **Figure 3:** Schematic lithostratigraphic column of the Paleoproterozoic formations of the Mako sector
 5 (Dabo et al., 2017). The thickness of the facies is estimated approximatively. From bottom to top it
 6 appears a mafic ophiolitic complex mainly of tholeiitic nature, topped by mixed volcanic complex
 7 with calc-alkali trend. The unit is intruded by three generations of granitoid (early, syn- and post-
 8 tectonic).

9 **Figure 4:** Aster radar image of Mako sector showing (a) in two (2D) dimensions orientation of the
 10 features and the rose diagram of the different directional features; (b) in three (3D) dimensions the
 11 morphological aspect with large overturned folds (P_1) whose hinges are re-folded (P_2). (c) and (d)
 12 correspond to the location of images of Figs. 6c,d. TH: Trace of syncline hinges.

13 **Figure 5:(a)** Pillowed metabasalts affected by a thrust fault, (b) and foliation S_1 affecting the normal
 14 limb of the overturned P_1 large fold within the metabasalts in pillows lavas. (c) Equal area projection,
 15 lower hemisphere, showing the position of the stretching lineation L_1 within S_1 foliation. (d) S_1
 16 foliation, stretching lineation L_1 (underlined by stretched pebbles and recrystallization of fine quartz
 17 grains along L_1 in the microphoto) and sigma clasts indicating a SE-NW overlapping in the
 18 quartzites. (e) Overturned bending P_1 folds affecting the metabasalts in pillow lavas. Cl: clast; TF:
 19 Thrust Fault.

20 **Figure 6:(a)** Metabasalts in pillow lavas showing high strain P_1 folds. (b) P_1 fold with curved axis in the
 21 metaperidotites. (c,d) Arcuate and flattening pillow lavas affected by P_1 mega-folds in the forelimb
 22 (c) and backlimb (d) of metabasalt hills. (e) Metabasalts in pillow lavas flattened and affected by
 23 shear joints and conjugate tension gashed indicating an NW-SE principal stress. (f) Equal area
 24 projection, lower hemisphere, showing conjugate shear fractures and their relation to the position of
 25 the principal stress. (g) Ptygmatic overturned folds highlighted by leucosome facies in the
 26 granodiorite of Soukourtou and cross-cut by S_2 foliation. (h) Metabasalt enclaves in Soukourtou
 27 granodiorite showing flower structure border (Cf) and locally stretched along L_1 stretching lineation
 28 direction.

29 **Figure 7:(a)** Bending of the trajectory of a NE-SW shear zone along with the N-S direction. (b) NW-SE
 30 shear zone affecting the tuffs of Bafoundou and showing two directions of foliation (S_{2a} , S_{2b}) and a
 31 stretching lineation L_2 underlined by the micro-pebbles stretching. (c) Shear zone showing a
 32 foliation S_1 - S_2 and a sinistral movement underlined by the bending of the pillow lavas. (d)
 33 S_{2a} foliation crenulated by S_{2c} foliation in the andesitic tuffs of Lamé. (e) Rhyolitic tuffs affecting a
 34 thrust-shear highlighted by a synkinematic fold (P_2) of the sinistral shear (XZ plane), stretching
 35 lineation (f) and delta clasts (XY plane) indicating a NE vergence.

36 **Figure 8:** Schematic block diagram of the structural evolution model of the Mako sector: (a)
 37 Eoeburnean D_1 phase with thrusting followed by (b) NW-SE sinistral reverse-shear zones; (c) early
 38 Eburnean D_2 phase which occurred after emplacement of intermediate to felsic rocks and is marked

1 by sinistral transpression responsible for the occurrence of NNW-SSE mylonitic corridor with
 2 stretching and boudinage of metaperidotites and quartzites ; **(d)** Eburnean D_3 phase characterized by
 3 dextral transtensional deformation which creates dextral shear zones and extensional structures
 4 (normal faults, grabens). Relations between **(b')** NE-SW reverse-shear zones and the principal stress
 5 during the D_1 deformation phase, **(c')** conjugated reverse-shear zones and the principal stress during
 6 the D_2 deformation phase, and **(d')** conjugated shear zones and the principal stress during the D_3
 7 deformation phase. EZ: extensional zone; Gb: graben; TC: "en-echelon" tension crack; CRF:
 8 conjugated reverse faults with a positive flower structure. 1: Ultramafic rocks, 2: Metagabbros, 3:
 9 Metabasalts, 4: Quartzites; 5-6: granitoids; 7-8: intermediateto felsic rocks; 9: silicified metabasalt
 10 with spotted gabbro injection in D_3 shear zones; 10-11: thrust fault and fault.

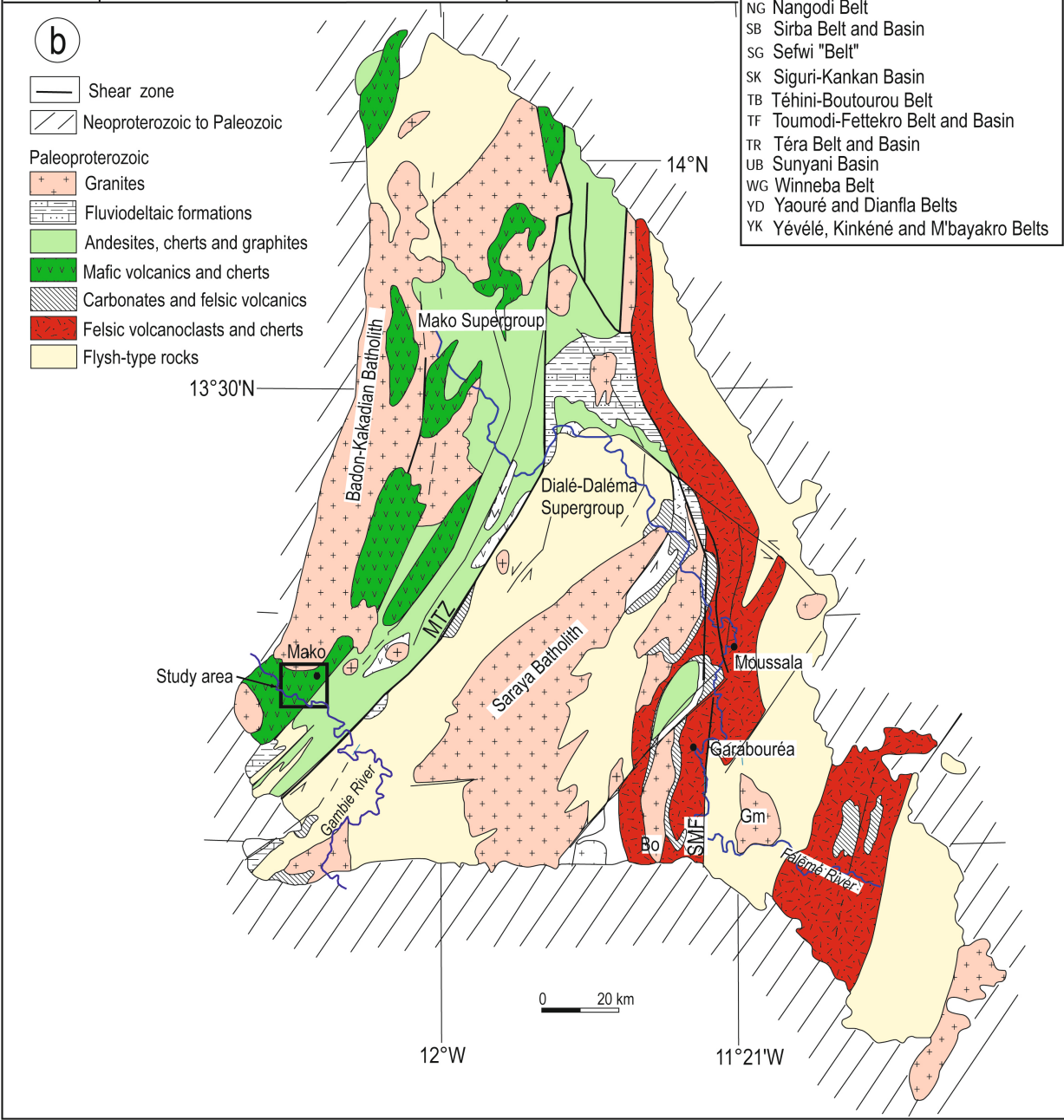
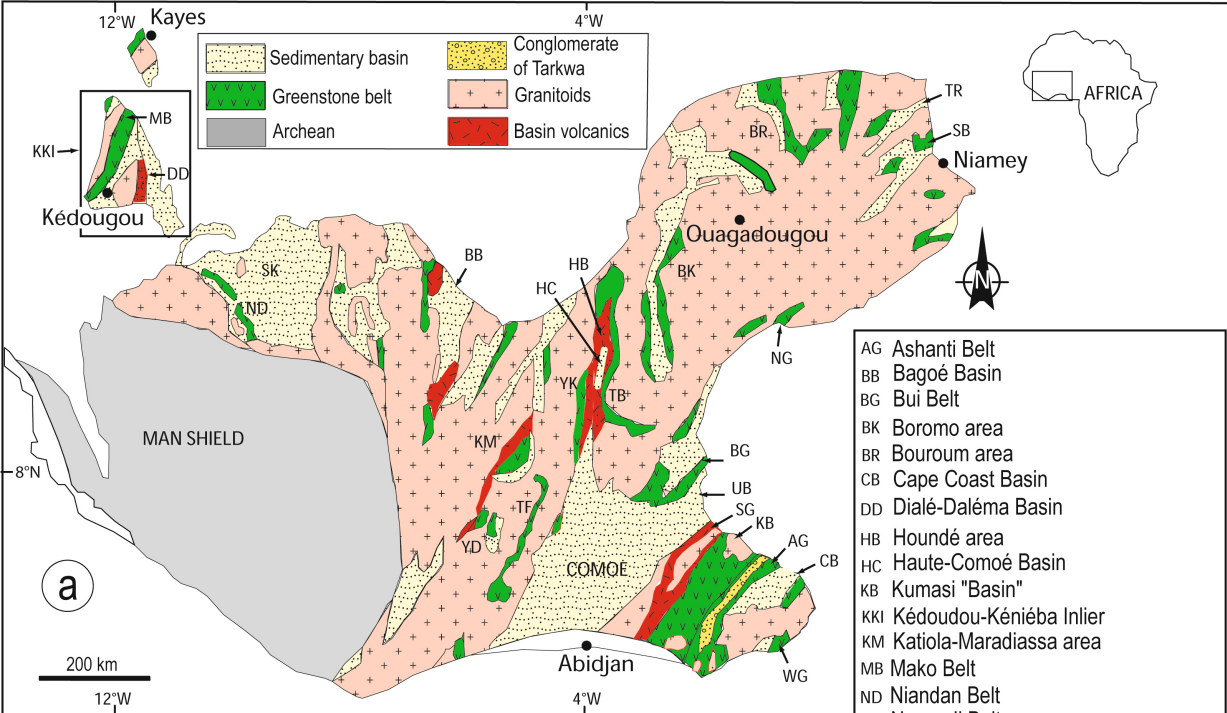
11 **Figure 9:**(a) Metagabbros affected by conjugate reverse faults (RF) which shifted a quartz vein (Qv)
 12 that underlined positive flower structure shape; **(b)** P_2 folds with tilted and short axis affecting the
 13 metagabbros;(c) Slickenlines in fault surface (slickenside); **(d)** The pitch and the fault surface
 14 plotted on a stereonet (equal area, lower hemisphere) showing the orientation of the principal stress;
 15 **(e)** Relics of synfolial folding in sinistral NNE-SSW shear zone related to D_2 deformation phase in
 16 the silicified metabasalts. **(f)** This same shear zone shows also synfolial folding and boudinage of
 17 felsic intrusion along S_3 foliation direction indicating a dextral shearing (D_3).

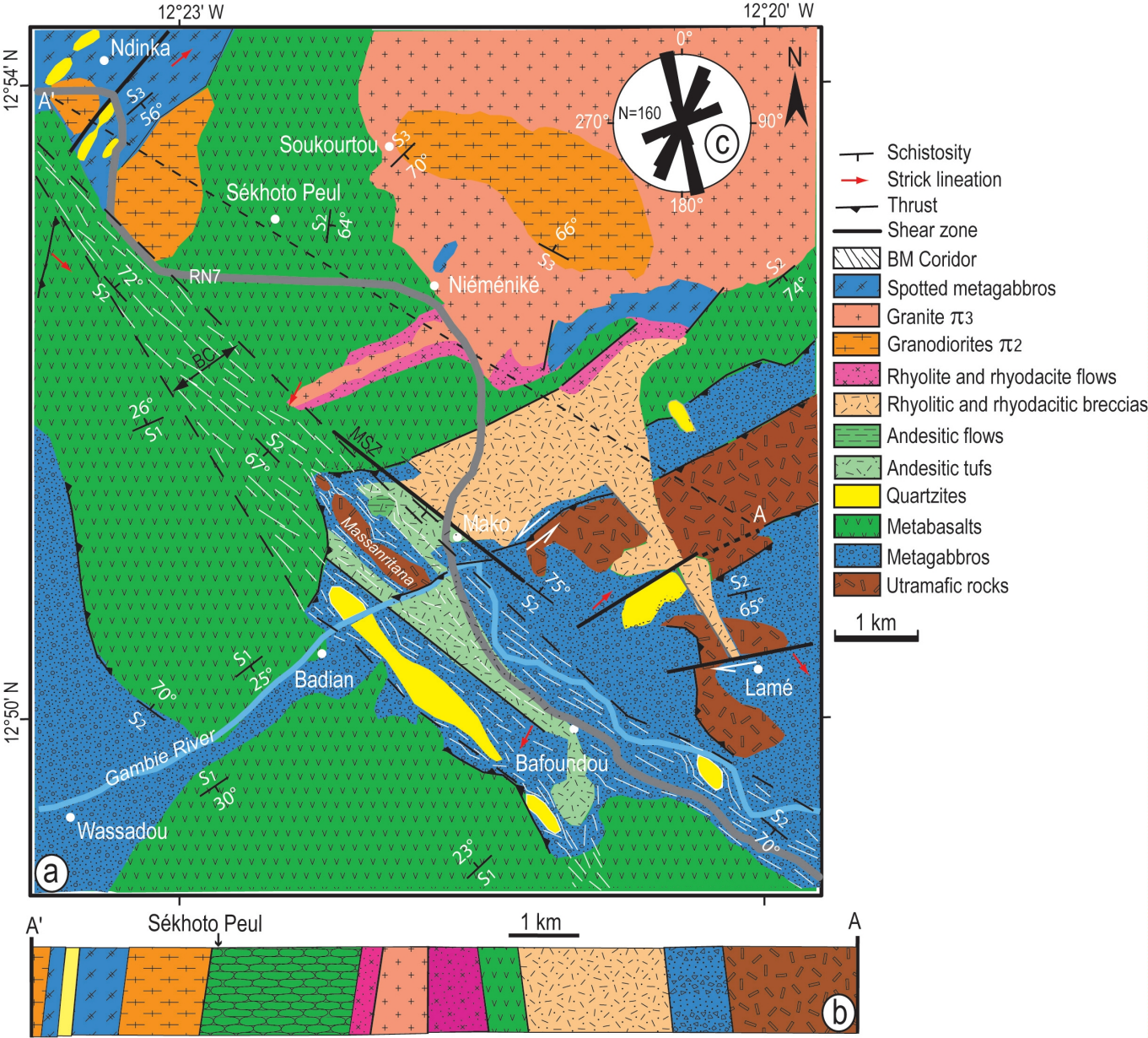
18 **Figure 10:**(a) S_3 foliation involving the S_{2b} foliation crenulation in the granite of Niéméniké; **(b)** S_3
 19 foliation involving the S_2 foliation crenulation in the NNW-SSE reverse-shear zone that affect the
 20 tuffs of Lamé; **(c)** "En-echelon" arranged extensional fractures related to normal faulting in the
 21 quartziticdiorite of Niéméniké; **(d,e)** Normal faults with opposite dips related to graben structure in
 22 the metaperidotites (Mp) and the tuffs (Tf); **(f)** Conjugate normal faults in the silicified metabasalts.

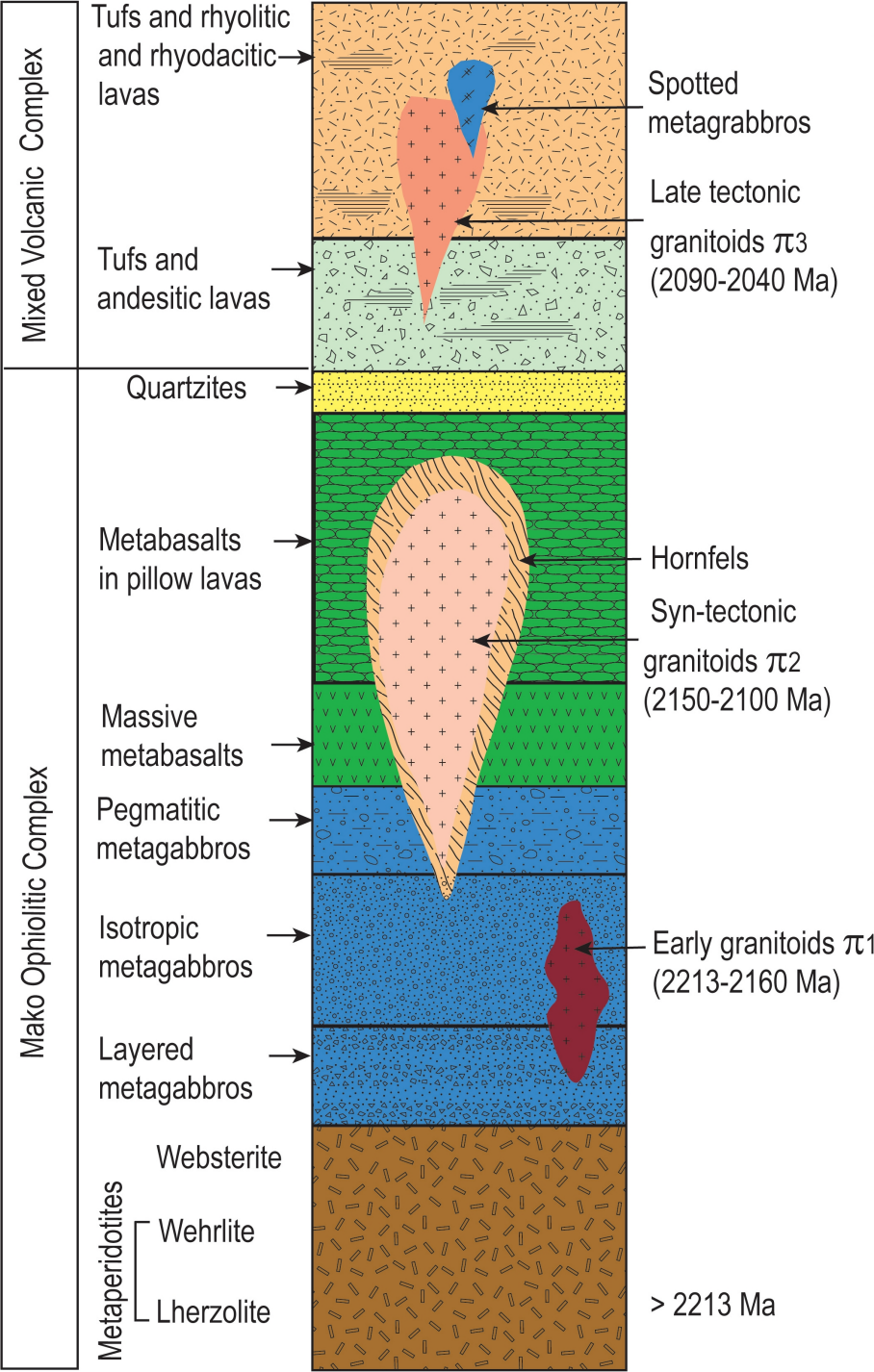
23

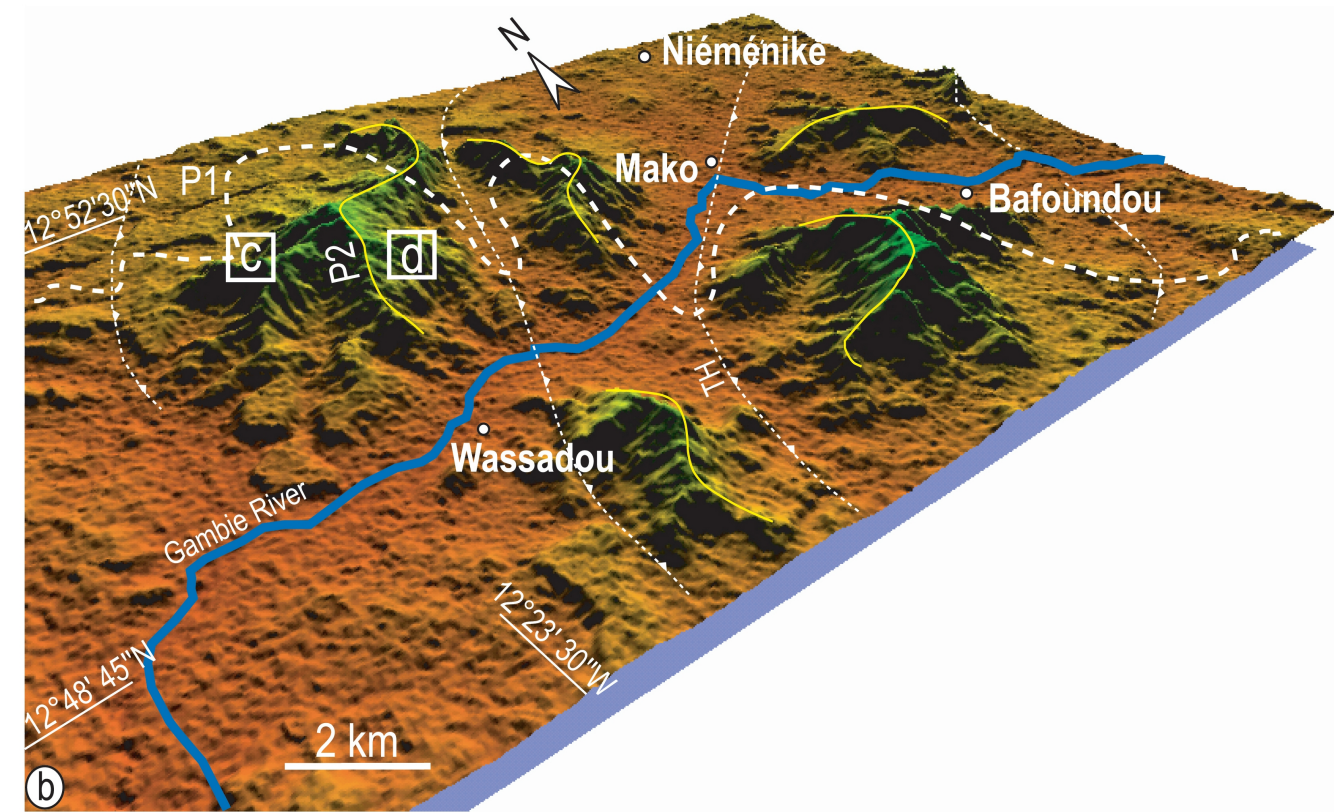
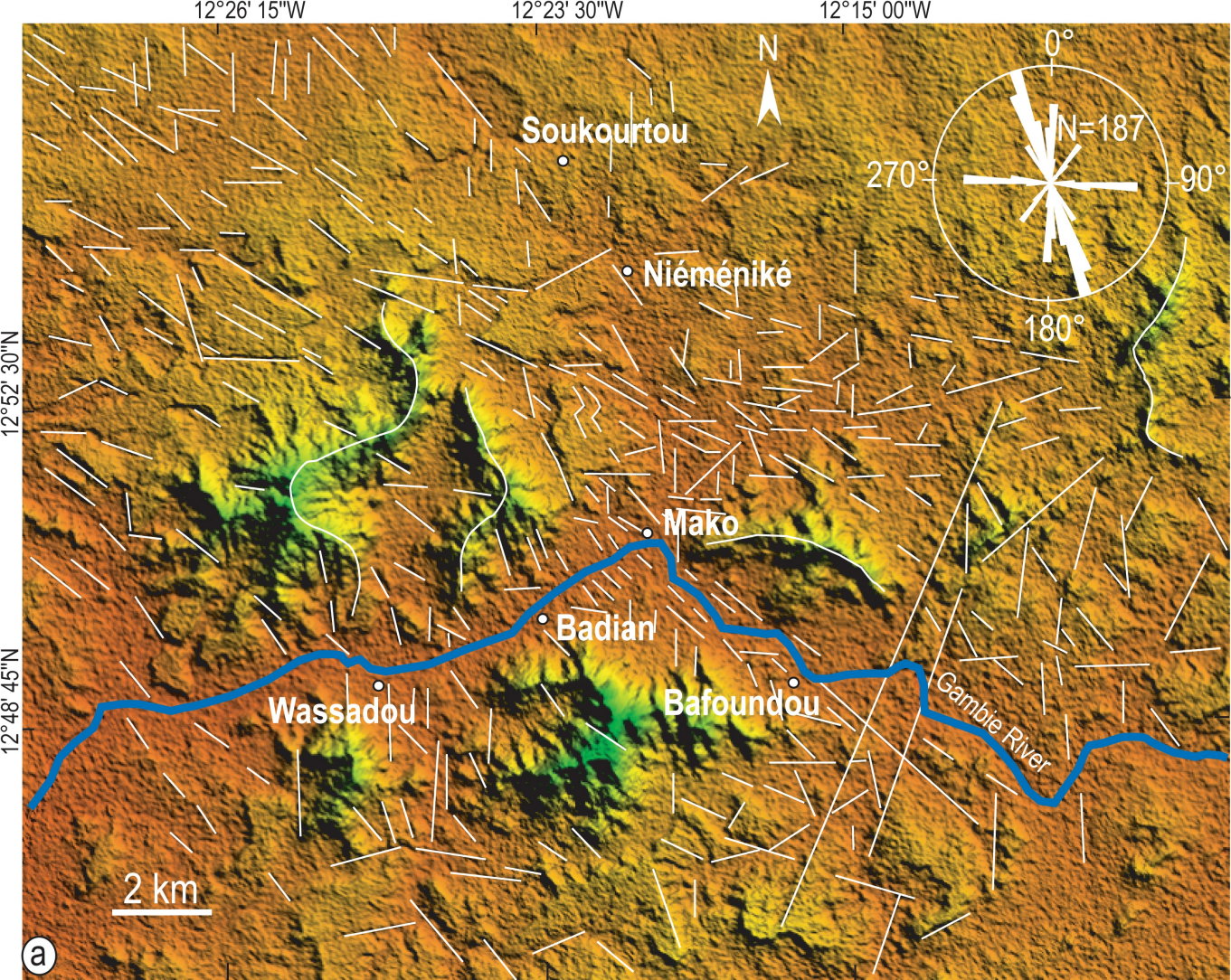
Highlights

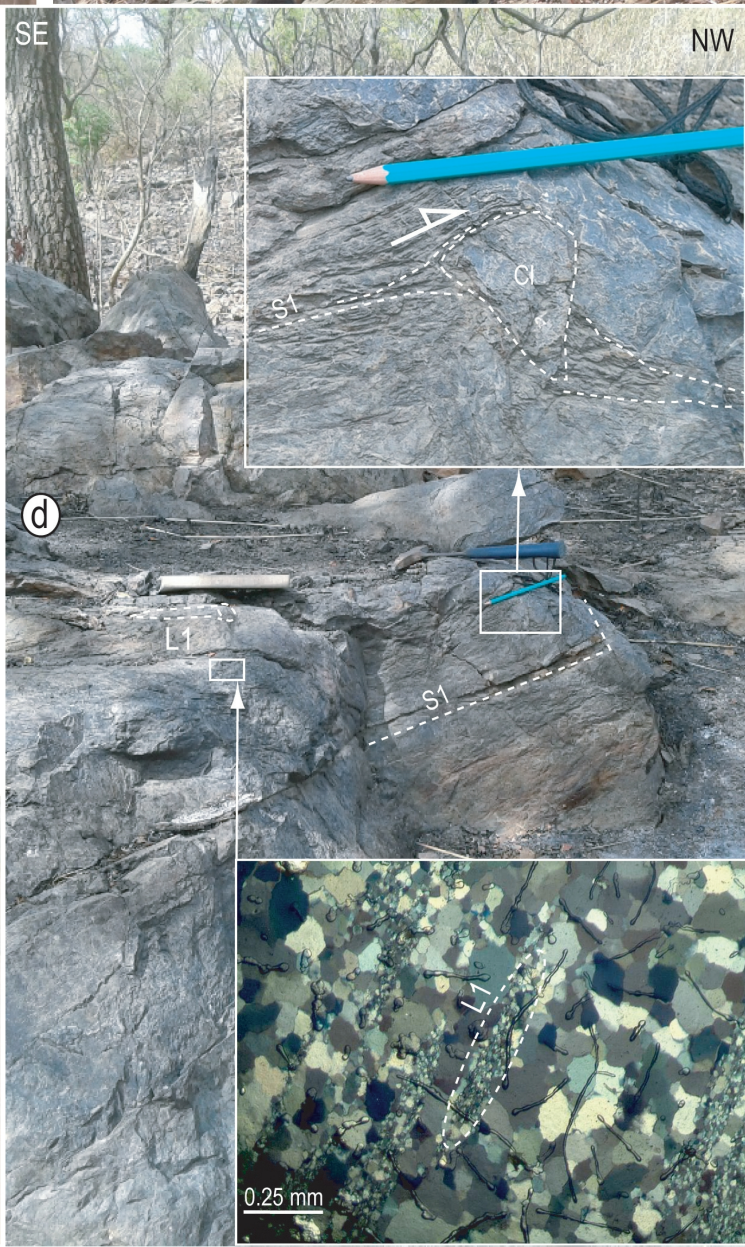
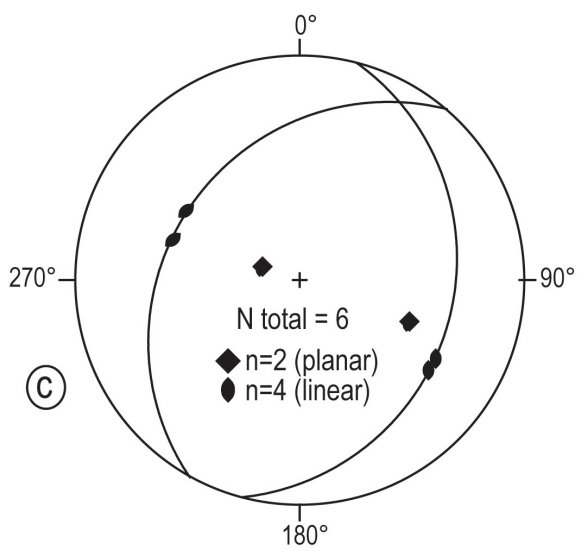
- Paleoproterozoic rocks of KKI were affected by Eoeburnean and Eburnean orogenic events with three deformation Phases.
- The Eoeburnean events are characterized by a compressive D₁ phase.
- Age of D₁ deformation deduced from emplacement of metabasalts in pillow lavas and the Badon granodiorite (c. 2198 Ma)
- The Eburnean event is marked by two deformation phases: transpressional D₂ followed by transtensional D₃.

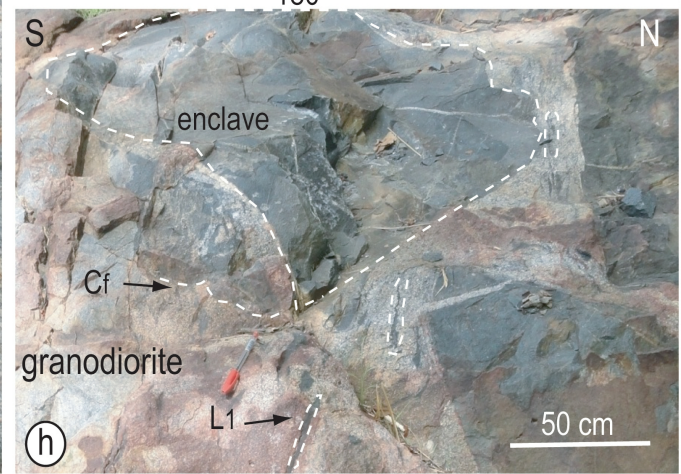
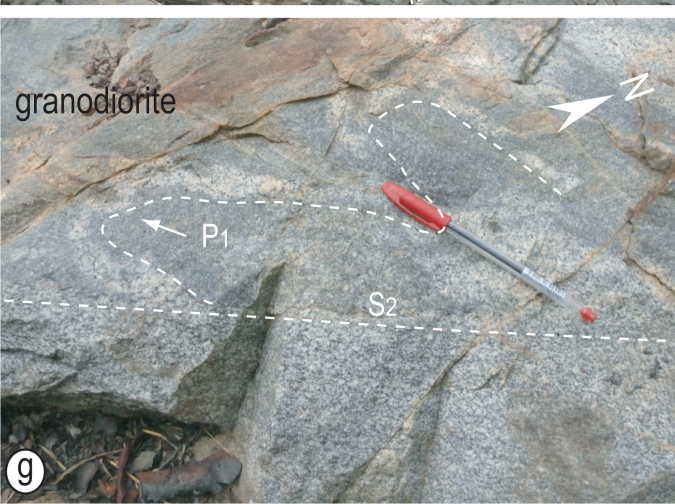
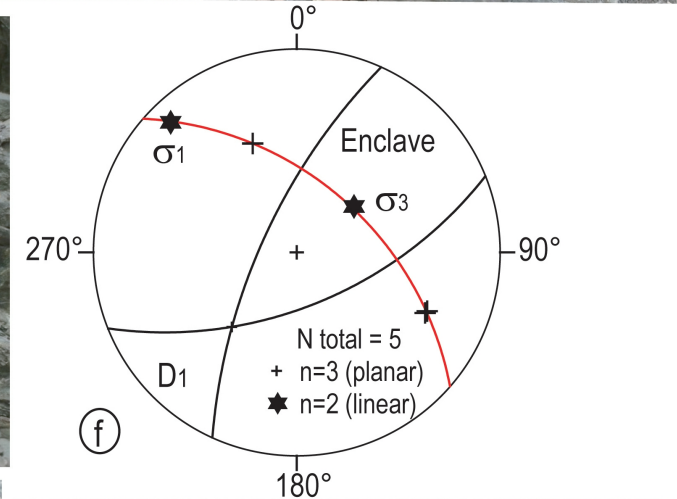
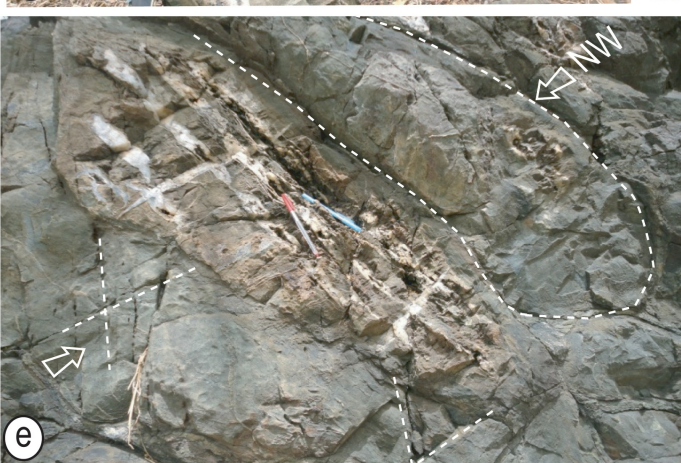
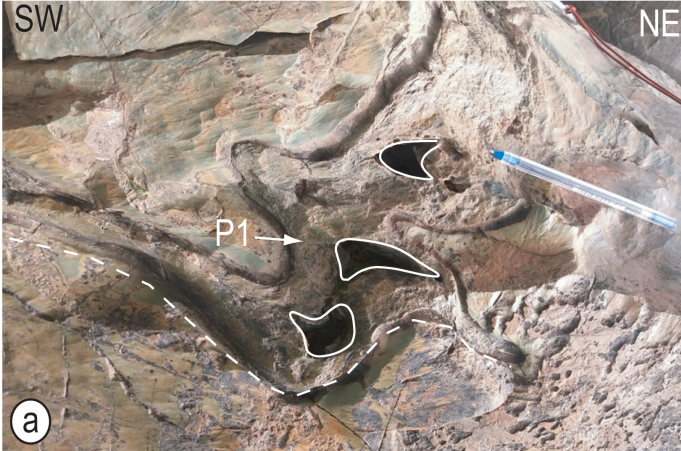


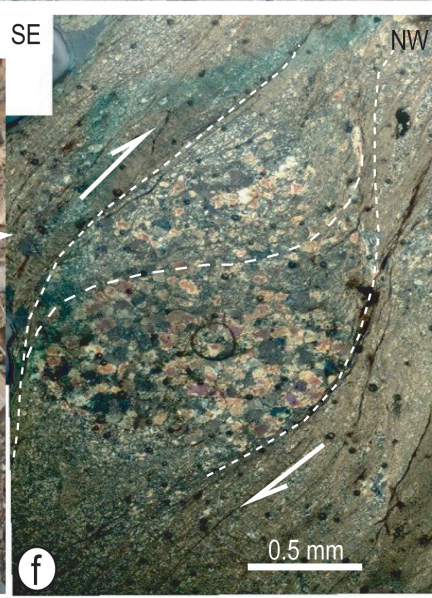
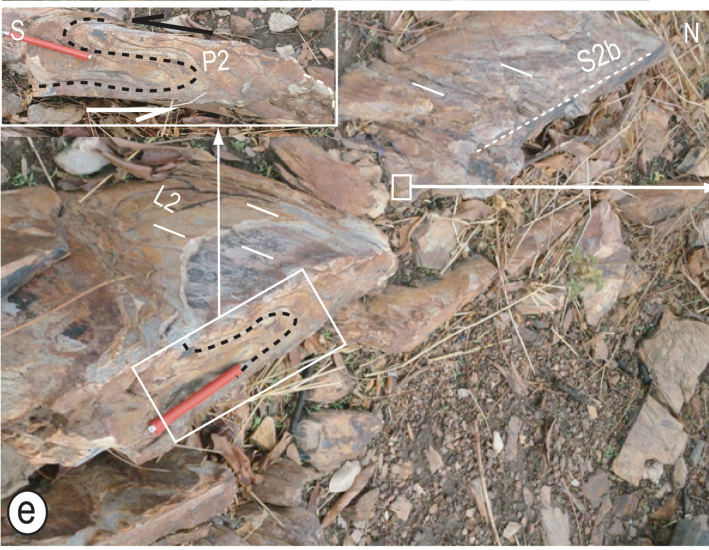


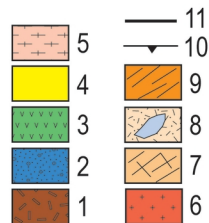
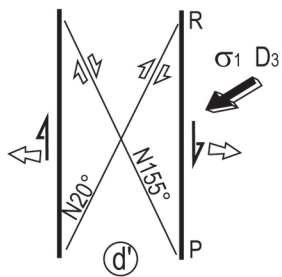
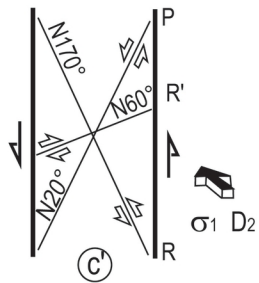
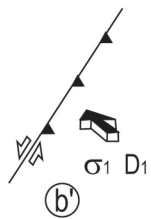
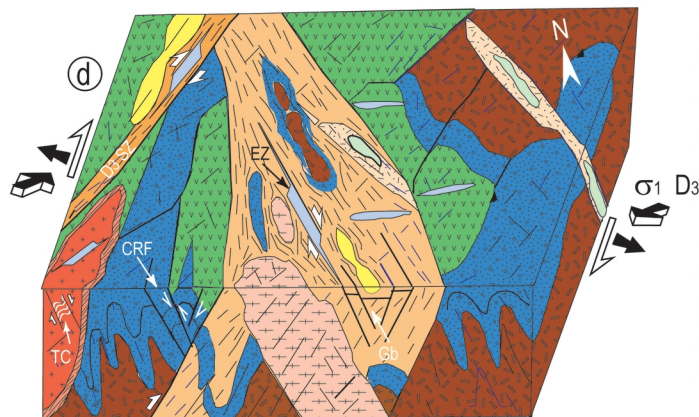
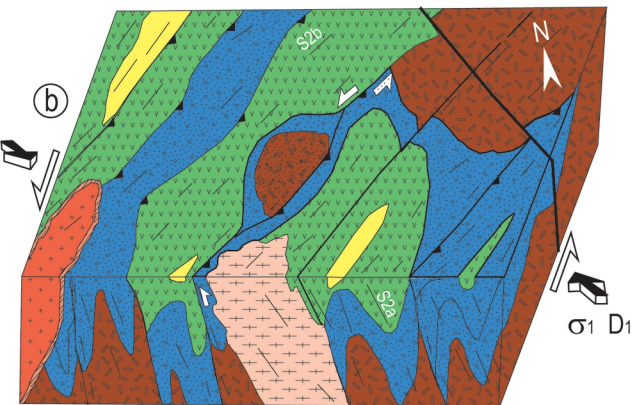
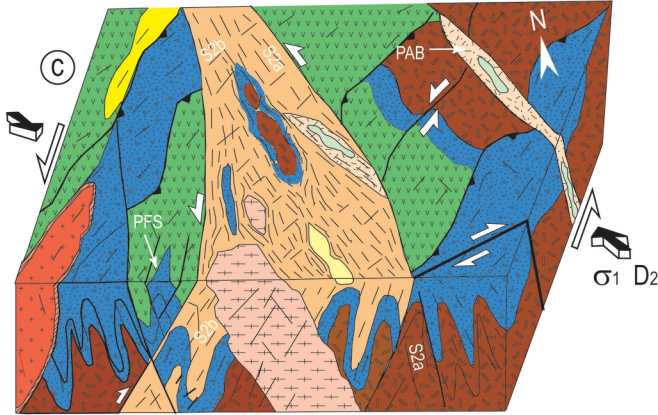
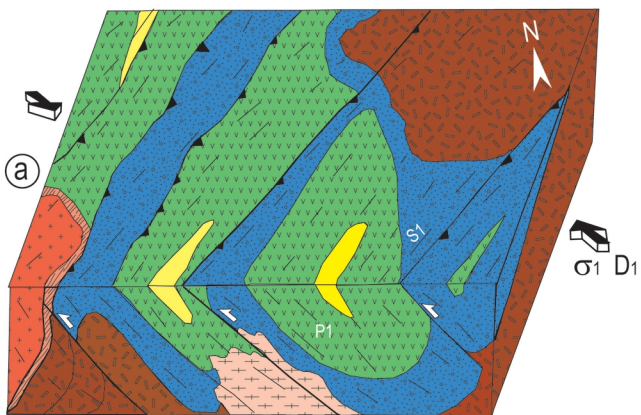


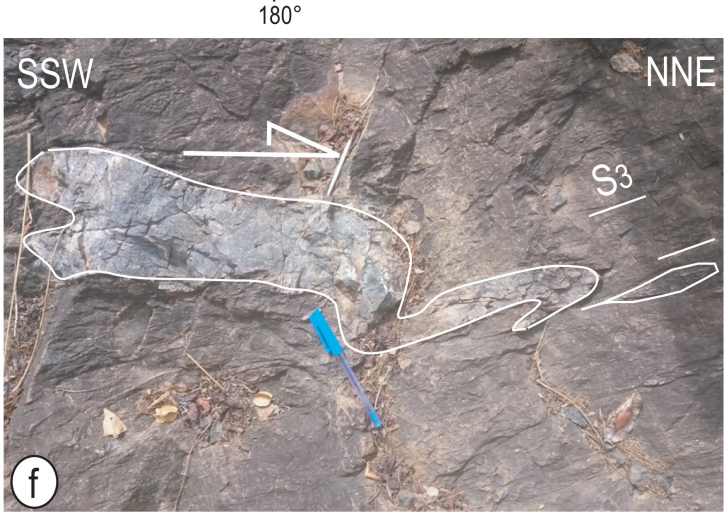
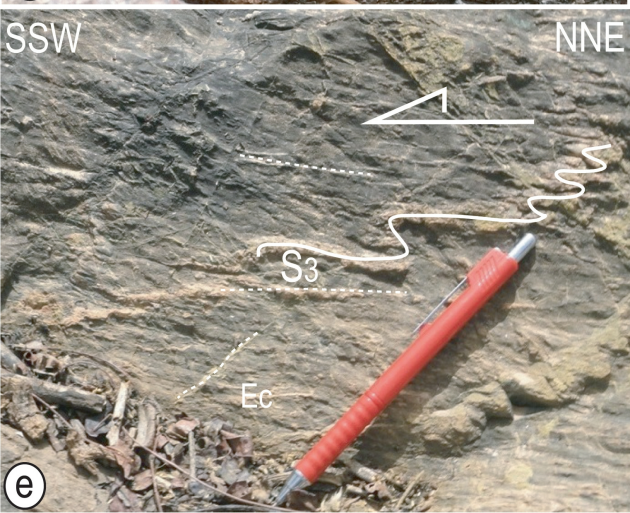
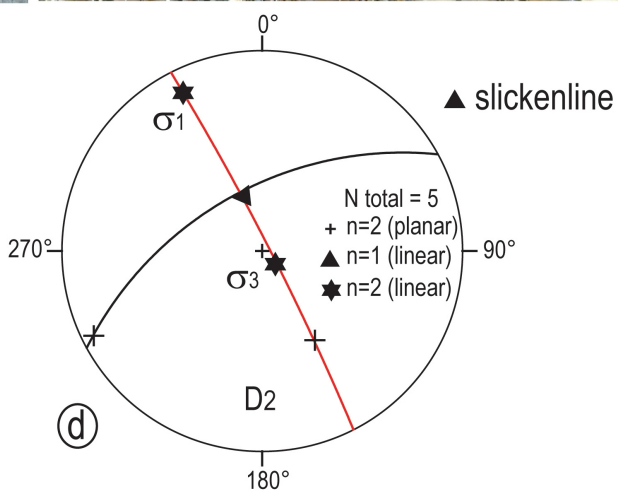
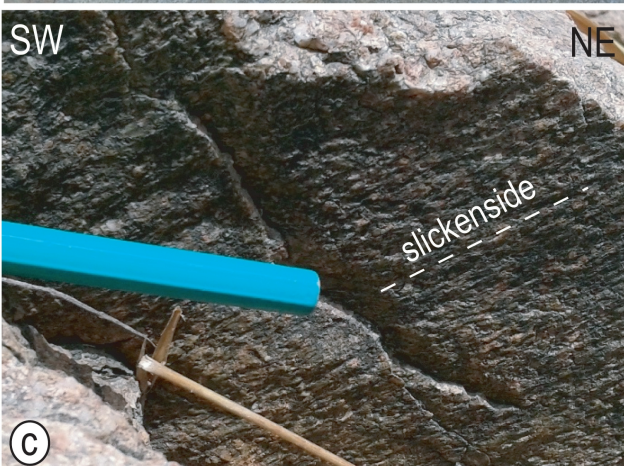
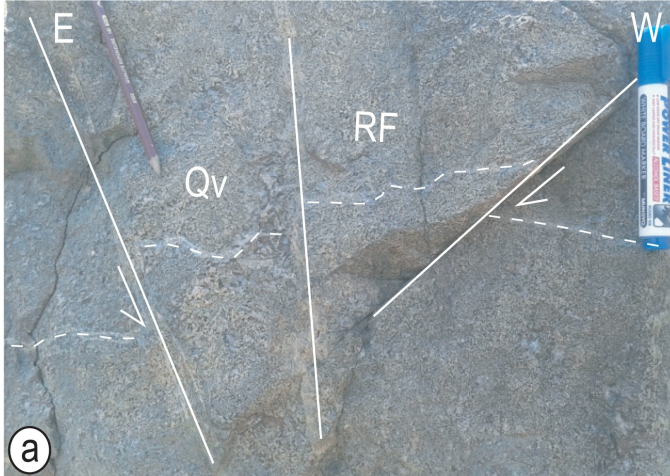












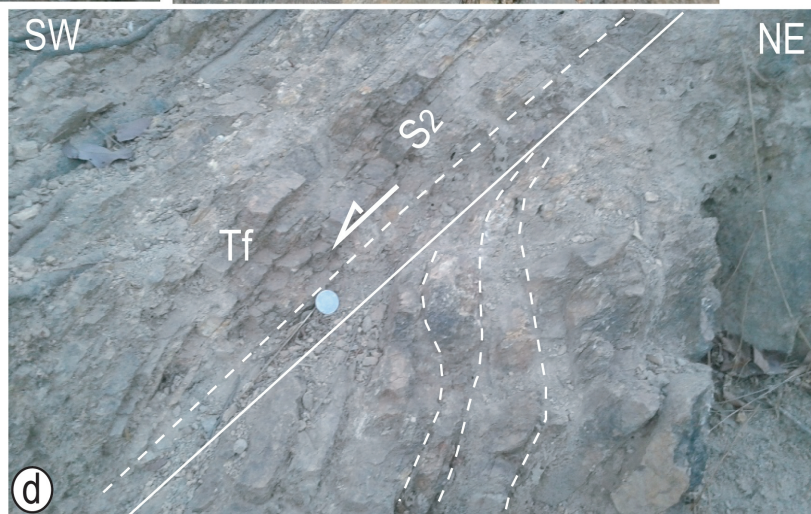
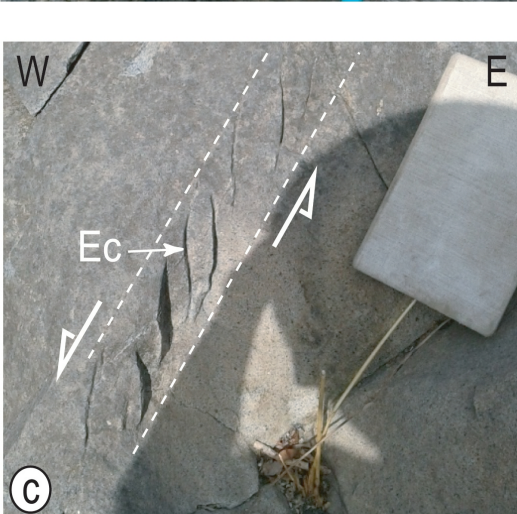
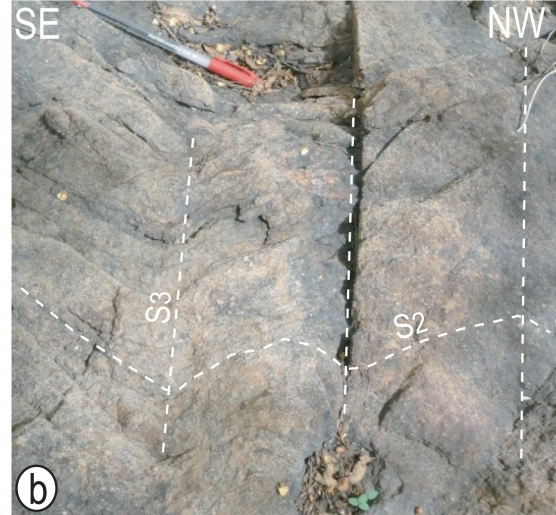
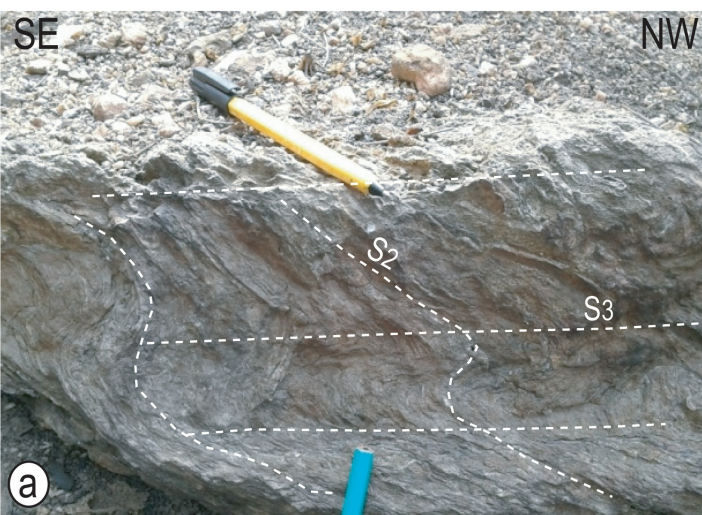


Table 1: Lithostratigraphy of the Birimian formations of KKI from bottom to top

	Bassot (1966)	Delor et al. (2010)	Ngom et al. (2011)
Dialé-Daléma Supergroup (top)	<ul style="list-style-type: none"> - Granitoids - Flysch - Cipolins, graywackes, quartzites, schists 	<ul style="list-style-type: none"> - Andesites, rhyodacites and volcano-sediments - Quartzites, sandstones - Graywackes, pelites, siltites - Carbonates 	<ul style="list-style-type: none"> - Granitoids 4 - Graywackes, sandstones, pelites - Pyroclastics - Andesitic flows - Graywackes, sandstones, pelites - Conglomerates
Mako Supergroup (bottom)	<ul style="list-style-type: none"> - Late mafic rocks - Granitoids - Flysch and conglomerates - Andesitics dominantly flows - Ophiolitic rocks 	<ul style="list-style-type: none"> - Volcano-sediments, sandstones, pelites and conglomerates - Rhyolite and rhyodacite - Basalts - Ultrabasic rocks 	<ul style="list-style-type: none"> - Granitoids 2 and 3 - Volcano-sediments - Massive felsics - Massive basalts - Sediments - Granitoids 1 - Peridotites - Pillowed basalts and jaspers

Table 2: Eoeburnean and Eburnean deformation phases in some Birimian provinces of the WAC

Authors	Study area	D ₁ deformation	D ₂ deformation	D ₃ deformation	D _{3+n} deformation
Delor et al. (2010)	Kédougou-Kéniéba, SE Senegal	Eoeburnean: peri-plutonic gravity driven deformations (2.17-2.14 Ga)	Eburnean Dt ₁ and Dt ₂ : transcurent tectonism		
Feybesse et al. (2006)	Regional Ghana	Trust tectonism (2.13 - 2.105 Ga)	D _{2,3} strike-slip movement (2.095 - 1.98 Ga)		
Block et al. (2015)	NW Ghana	NS horizontal shortening with reverse shear zones	NS extensional shearing	EW shortening and N to NNE stretching	D ₄ -D ₇ narrow shear zones in dominantly transcurent regime